# Long Distance Wireless Radio Frequency Link for the ITS Statewide Network

# FDOT Contract Number: BDV34-977-08

## Final Report

**Submitted To:**

Research Center
Florida Department of Transportation
and
Project Manager: Allen Skinner
Florida Department of Transportation

**Submitted By:**

Principal Investigator: Brian Kopp, Ph.D.
University of North Florida
School of Engineering
Building 4, Room 3010
Jacksonville, FL 32224

**December 2020**

DISCLAIMER PAGE

The opinions, findings, and conclusions expressed in this publication are those of the authors and not necessarily those of the Florida Department of Transportation.

The contents of this report reflect the views of the authors, who are responsible for the facts and the accuracy of the information presented herein. This document is disseminated under the sponsorship of the Department of Transportation's University Transportation Centers Program, in the interest of information exchange. The U.S. Government assumes no liability of the contents or use thereof.

APPROXIMATE CONVERSIONS TO SI UNITS

| SYMBOL | WHEN YOU KNOW | MULTIPLY BY | TO FIND | SYMBOL |
|---|---|---|---|---|
| LENGTH | | | | |
| in | inches | 25.4 | millimeters | mm |
| ft | feet | 0.305 | meters | m |
| yd | yards | 0.914 | meters | m |
| mi | miles | 1.61 | kilometers | km |
| **SYMBOL** | **WHEN YOU KNOW** | **MULTIPLY BY** | **TO FIND** | **SYMBOL** |
| AREA | | | | |
| $in^2$ | square inches | 645.2 | square millimeters | $mm^2$ |
| $ft^2$ | square feet | 0.093 | square meters | $m^2$ |
| $yd^2$ | square yard | 0.836 | square meters | $m^2$ |
| ac | acres | 0.405 | hectares | ha |
| $mi^2$ | square miles | 2.59 | square kilometers | $km^2$ |
| **SYMBOL** | **WHEN YOU KNOW** | **MULTIPLY BY** | **TO FIND** | **SYMBOL** |
| VOLUME | | | | |
| fl oz | fluid ounces | 29.57 | milliliters | mL |
| gal | gallons | 3.785 | liters | L |
| $ft^3$ | cubic feet | 0.028 | cubic meters | $m^3$ |
| $yd^3$ | cubic yards | 0.765 | cubic meters | $m^3$ |
| NOTE: volumes greater than 1000 L shall be shown in $m^3$ | | | | |
| **SYMBOL** | **WHEN YOU KNOW** | **MULTIPLY BY** | **TO FIND** | **SYMBOL** |
| MASS | | | | |
| oz | ounces | 28.35 | grams | g |
| lb | pounds | 0.454 | kilograms | kg |
| T | short tons (2000 lb) | 0.907 | megagrams (or "metric ton") | Mg (or "t") |
| **SYMBOL** | **WHEN YOU KNOW** | **MULTIPLY BY** | **TO FIND** | **SYMBOL** |
| TEMPERATURE (exact degrees) | | | | |
| ºF | Fahrenheit | 5 (F-32)/9<br>or (F-32)/1.8 | Celsius | ºC |
| **SYMBOL** | **WHEN YOU KNOW** | **MULTIPLY BY** | **TO FIND** | **SYMBOL** |
| ILLUMINATION | | | | |
| fc | foot-candles | 10.76 | lux | lx |
| fl | foot-Lamberts | 3.426 | candela/$m^2$ | cd/$m^2$ |
| **SYMBOL** | **WHEN YOU KNOW** | **MULTIPLY BY** | **TO FIND** | **SYMBOL** |
| FORCE and PRESSURE or STRESS | | | | |
| lbf | pound force | 4.45 | newtons | N |
| lbf/$in^2$ | pound force per square inch | 6.89 | kilopascals | kPa |

APPROXIMATE CONVERSIONS TO ENGLISH UNITS

| SYMBOL | WHEN YOU KNOW | MULTIPLY BY | TO FIND | SYMBOL |
|---|---|---|---|---|
| | | LENGTH | | |
| mm | millimeters | 0.039 | inches | in |
| m | meters | 3.28 | feet | ft |
| m | meters | 1.09 | yards | yd |
| km | kilometers | 0.621 | miles | mi |
| **SYMBOL** | **WHEN YOU KNOW** | **MULTIPLY BY** | **TO FIND** | **SYMBOL** |
| | | AREA | | |
| $mm^2$ | square millimeters | 0.0016 | square inches | $in^2$ |
| $m^2$ | square meters | 10.764 | square feet | $ft^2$ |
| $m^2$ | square meters | 1.195 | square yards | $yd^2$ |
| ha | hectares | 2.47 | acres | ac |
| $km^2$ | square kilometers | 0.386 | square miles | $mi^2$ |
| **SYMBOL** | **WHEN YOU KNOW** | **MULTIPLY BY** | **TO FIND** | **SYMBOL** |
| | | VOLUME | | |
| mL | milliliters | 0.034 | fluid ounces | fl oz |
| L | liters | 0.264 | gallons | gal |
| $m^3$ | cubic meters | 35.314 | cubic feet | $ft^3$ |
| $m^3$ | cubic meters | 1.307 | cubic yards | $yd^3$ |
| **SYMBOL** | **WHEN YOU KNOW** | **MULTIPLY BY** | **TO FIND** | **SYMBOL** |
| | | MASS | | |
| g | grams | 0.035 | ounces | oz |
| kg | kilograms | 2.202 | pounds | lb |
| Mg (or "t") | megagrams (or "metric ton") | 1.103 | short tons (2000 lb) | T |
| **SYMBOL** | **WHEN YOU KNOW** | **MULTIPLY BY** | **TO FIND** | **SYMBOL** |
| | | TEMPERATURE (exact degrees) | | |
| $^oC$ | Celsius | 1.8C+32 | Fahrenheit | $^oF$ |
| **SYMBOL** | **WHEN YOU KNOW** | **MULTIPLY BY** | **TO FIND** | **SYMBOL** |
| | | ILLUMINATION | | |
| lx | lux | 0.0929 | foot-candles | fc |
| $cd/m^2$ | candela/$m^2$ | 0.2919 | foot-Lamberts | fl |
| **SYMBOL** | **WHEN YOU KNOW** | **MULTIPLY BY** | **TO FIND** | **SYMBOL** |
| | | FORCE and PRESSURE or STRESS | | |
| N | newtons | 0.225 | pound force | lbf |
| kPa | kilopascals | 0.145 | pound force per square inch | $lbf/in^2$ |

TECHNICAL REPORT DOCUMENTATION PAGE

| 1. Report No. | 2. Government Accession No. | 3. Recipient's Catalog No. |
|---|---|---|
| 4. Title and Subtitle<br>Long Distance Wireless Radio Frequency Link for the ITS Statewide Network | | 5. Report Date<br>December 2020<br>6. Performing Organization Code |
| 7. Author(s)<br>Brian Kopp | | 8. Performing Organization Report No. |
| 9. Performing Organization Name and Address<br>University of North Florida<br>1 UNF Drive<br>Jacksonville, FL 32224 | | 10. Work Unit No. (TRAIS)<br>11. Contract or Grant No.<br>BDV34-977-08 |
| 12. Sponsoring Agency Name and Address<br>Florida Department of Transportation<br>605 Suwannee Street, MS 30<br>Tallahassee, FL 32399 | | 13. Type of Report and Period Covered<br>Final Report<br>April 2016 – December 2020<br>14. Sponsoring Agency Code |
| 15. Supplementary Notes | | |

16. Abstract

This project began an investigation into whether it is possible to create a useful microwave communications link across the Gulf of Mexico in order to link the linear Florida Department of Transportation networks in the Florida Keys and Florida Panhandle, creating network redundancy for the first time for both segments. The work in this project has involved the design, procurement, construction, and initial testing of the equipment that will be used to conduct propagation testing under a future project. Originally the scope included the final stage of testing and the actual propagation tests. However, due to project delays, temporary university travel restrictions, and FDOT equipment scheduling issues, the scope was reduced to include only the tasks listed above. All of the work in the revised scope has been completed successfully. A future project will execute the final integrated system testing and deploy the equipment for actual field tests.

| 17. Key Word | 18. Distribution Statement |
|---|---|
| Beyond line of sight microwave communications, propagation, wireless, networks | No Restrictions. |

| 19. Security Classif. (of this report) | 20. Security Classif. (of this page) | 21. No. of Pages | 22. Price |
|---|---|---|---|
| Unclassified. | Unclassified. | 53 | |

**Form DOT F 1700.7** (8-72) Reproduction of completed page authorized

# EXECUTIVE SUMMARY

This final report summarizes all research and results for the FDOT project entitled “Long Distance Wireless Radio Frequency Link for the ITS Statewide Network.” During this effort, the design, component procurement, construction, and initial testing of the equipment for two portable microwave propagation test stands was completed.

This initial project began the investigation to determine whether the use of an over-water wireless microwave propagation methodology could help alleviate the FDOT intelligent transportation system statewide network path vulnerabilities that exist in the Florida Keys and the Florida Panhandle. The project approach was to first research the topic with a literature search. Next, two portable microwave test stations were designed. The components for the design were then procured. When the components were received, the main microwave transmitter and receiver systems were constructed. This initial project concluded with the successful testing of these two systems. These tasks are the subject of this report.

The original project scope included the follow-on tasks of integration and field testing, but working with FDOT, it was determined that this initial project should be considered completed after the subsystem testing task. The original project schedule was impacted by procurement delays and an underestimate of the amount of time necessary for undergraduate student researchers to construct the sophisticated and complex microwave test stations. In addition, at the start of the project, the plan was to use two FDOT trailers for the portable test stations. Several years after the start of the project, one of the trailers was no longer available when the mobile station integration work was to begin. To continue would have required the research team to identify another FDOT trailer asset and redesign that station for that new trailer. The final reason it was decided to split the project into this initial project and a future project was that the University of North Florida instituted travel bans for faculty and student researchers in early 2020 during the pandemic. This created an indefinite delay on the project as the five-year FDOT project maximum limit of early 2021 was approaching.

A future research project will be proposed to the FDOT to complete the project by first integrating the transmitter and receiver systems into the microwave test stations, and then conducting the field tests with the transmitter microwave test station positioned in the lower Florida Keys and the receiver microwave test station positioned near the western end of the Florida Panhandle. It is hoped a radio link will be established between the two sites that is of sufficient reliability to warrant building a permanent link and interconnecting with the existing statewide network.

TABLE OF CONTENTS

LIST OF FIGURES

LIST OF TABLES

# CHAPTER 1. INTRODUCTION

The Florida Department of Transportation (FDOT) Intelligent Transportation System (ITS) statewide network supports mission critical applications throughout the state, including, for instance, voice radio and video applications. Whereever possible, this statewide network has been built to support operations even when there are equipment failures or network outages due to either man-made or natural events such as hurricanes. To help achieve this resilience, the network is deployed with redundant paths that are physically separate from each other so that communication signals have alternative connections available between any two points in the network. If one path suffers an outage, the alternate path can complete the connection. This is in part why there are microwave and fiber circuits on both sides of the state along interstates I-75 and I-95.

Currently, there are two regions of the state where this redundancy is not possible because of geography. One region is the panhandle of Florida, from Pensacola to Lake City. The other region is the Florida Keys. Both of these regions have long narrow geographies that prevent the installation of physically separate network paths. It would be desirable to alleviate all or part of these vulnerabilities, thereby improving network reliability so that these regions of the FDOT ITS statewide network are not completely cut off from the rest of the state in the event of an equipment failure or network outage.

A potential solution exists that FDOT may be able to use to provide an alternative path for these two geographically challenged regions of the ITS statewide network. There has been recent research work in the use of wireless radio frequency (RF) transmission on over-water paths that are considered long-distance and beyond-line-of-sight because they are over the horizon. It may be possible to utilize this method of communications to establish a link between locations in the Florida Keys and the panhandle of Florida. Providing network connections between these locations could provide redundant and physically separate paths for the ITS statewide network and better serve both of these regions.

This initial project began the investigation to determine whether the use of this over-water wireless RF propagation methodology could help alleviate the FDOT ITS statewide network path vulnerabilities. The project approach was to first research the topic with a literature search. Next, two portable microwave test stations were designed. The components for the design were then procured. When the components were received, the construction of the main microwave RF transmitter and receiver systems was commenced. This initial project concluded with the successful testing of these systems. A future research project will be proposed to the FDOT to complete the project by first integrating the transmitter and receiver systems into the microwave test stations, and then conducting the field tests with the transmitter microwave test station positioned in the lower Florida Keys and the receiver microwave test station positioned near the western end of the Florida Panhandle.

The original project scope included the integration and field testing but, working with FDOT, it was determined that this initial project should be considered completed after the subsystem testing task. The original project schedule was impacted by procurement delays and an underestimate of the amount of time necessary for undergraduate student researchers to construct the sophisticated and complex microwave test stations. In addition, at the start of the project, the plan was to use two FDOT trailers for the portable test stations. Several years after the start of the project, one of the trailers was no longer available when the mobile station integration work was to begin. To continue would have required the research team to identify another FDOT trailer asset and redesign that station for that new trailer. The final reason it was decided to split the project into this initial project and a future project was that the University of North Florida instituted travel bans for faculty and student researchers in early 2020 during the pandemic. This created an indefinite delay on the project as the five-year FDOT project maximum limit of early 2021was approaching.

The report is organized according to the tasks that were executed. The literature search results for task 1 are presented first in Chapter 2. The design in Task 2 is presented next in Chapter 3. Chapter 4 discusses the procurement covered in Task 3 and the Chapter 5 presents the construction and testing work conducted in Task 4. The conclusions and a discussion on the follow-on project are presented in Chapter 6, with references and appendices at the end of the report.

# CHAPTER 2. LITERATURE SEARCH

Wireless signals propagate through a vacuum in a straight line. The earth's atmosphere causes these wireless signals to bend in a process called refraction. The amount of bending in the atmosphere is described by the rate of change of this refraction with altitude, and is called the refractivity gradient. Different values of positive refractive gradient are categorized as sub refraction, standard refraction, and super refraction. With sub refraction the signal is actually bent away from the earth, a condition that is not of use for b-LoS communications. However, when the signal is bent toward the earth by the atmosphere, it appears to travel somewhat parallel to the earth suggesting there is a "duct" that is permitting the signal to remain close to the earth. This is the case for standard and super refraction. In both cases though, the amount of bending is not enough to follow the curvature of the earth and so the duct will slowly separate away from the earth as it propagates along the duct. There is a fourth category for the refractivity gradient and that is when it is negative. In that case, the signal is bent toward the earth and said to be under a trapping refractivity condition. This fourth category is of particular interest for b-LoS communications. Under the trapping condition, signals can skip off the earth and then repeatedly bend back toward it as they propagate over the horizon. If the earth is highly reflective (a condition that can occur with over-water links) then the reflected signals will remain strong, even after multiple reflections. Therefore, if the trapping refractivity condition exists over long water paths then it is possible to provide a duct near the surface of the water for signals to propagate along without suffering the losses associated with even a comparable Line-of-Sight LoS propagation path.

These conductive atmospheric ducts can occur with regularity in atmospheric regions that are experiencing high evaporative rates, such as an air-sea interface (Dinc & Akan, 2014), (Rottier et al., 2001), and (Gadwal & Barrios, 2009). The duct just above the surface of the sea is referred to as the Evaporative Duct and occurs in the first few meters of atmosphere where the humidity decreases rapidly. This phenomenon suggests that more equatorial regions would experience more reliable evaporative duct formation because of increased humidity. However, these evaporative ducts have been verified to occur at latitudes including 16° south on the Great Barrier Reef (Woods et al., 2009) and 21° North off the coast of Oahu, Hawaii (Anderson et al., 2003) as well as the South China Sea (Yang et al., 2015).

To date, research on this topic has focused on modelling the evaporative duct using either Parabolic Equations (PE) or ray optics (Dinc & Akan, 2014). The United States Navy's Space and Naval Warfare Systems Center in San Diego, California has developed one of the models used for estimating duct performance (a hybrid model that uses both PE and ray optics), called the "Advanced Refractive Effects Prediction System" (AREPS) (Patterson, 2007) and (Frederickson, 2016). A second model, available to the public, is called PETOOLS (Ozgun et al., 2011). It uses PE to model propagation. Besides modelling, the two experimental research efforts in Australia and Hawaii, mentioned above, are among the very few unclassified studies that have published actual test results recently (Babin et al., 1997). Only a few projects have discussed the construction of any test configurations and hardware that may be useful for the current project or for extending it (Kerans et al., 2010), (Luddy et al., 2011) and (Hansen et al., 2011).

The publications identified in this literature search are all presented in the reference section at the end of this report and are also listed below where they are discussed in detail.

Article Number: 1

Author(s): Ergin Dinc and Ozgur B. Aka

Title: Beyond-Line-of-Sight Communications with Ducting Layer

Source: IEEE Communications Magazine, October, 2014, pgs. 37-43

Summary: Overview article on the use of maritime evaporative ducts at sea-level to propagate microwave signals over the horizon. The microwave channel is discussed as well as scientific models in use for the channel. Open areas of research are discussed and network-centric applications that can take advantage of over the horizon (beyond line of sight) communications.

FDOT Project Relevance: This article is an excellent source for quickly becoming familiar with the topic of the research project. It also referred to research by the United States Navy that suggests the proposed 500 mile link in this FDOT project may be possible.

Article Number: 2

Author(s): Graham S. Woods, Adam Ruxton, Cameron Huddlestone-Holmes, and Gilles Gigan

Title: High-Capacity, Long-Range, Over Ocean Microwave Link Using the Evaporation Duct

Source: IEEE Journal of Oceanic Engineering, Volume 34, Number 3, July 2009, pgs. 323-330

Summary: This article reviews an experimental evaporative duct microwave link set up on the Great Barrier Reef in Australia. Using a 10.6 GHz microwave path, a 10 Mbps link was achieved over a distance of 78 km. Data is presented over a three week period in August (winter in the southern hemisphere) and reported availabilities ranged from 50% to 100%, averaging 80%.

FDOT Project Relevance: These experimental results will be used to help design the current project's experimental links. They will also serve as comparative data.

Article Number: 3

Author(s): Steven M. Babin, George S. Young, and James A. Carton

Title: A New Model of the Oceanic Evaporation Duct

Source: Journal of Applied Meteorology, Volume 36, March 1997, pgs. 193-204

Summary: This article reviews two current models of the evaporative duct and then proposes a third model that improves upon issues in the current models. Experimental data was gathered to validate the new model. The experimental data suggests the new model has a 3 meter RMS error which is better than that of the current US Navy's model (4.3 meter error) or the current European model (13.1 meter error). The experimental data was collected off Wallops Island Virginia and in the tidal Potomac River. The data trended toward a 5-10 meter duct height off Wallops Island and a 10-15 meter duct height in the tidal Potomac River.

FDOT Project Relevance: The experimental data will be used to help set up the experiments in this project. The evaporative duct model may prove useful for verifying results and predicting outcomes from the experiments.

Article Number: 4

Author(s): A. J. Kerans, A. S. Kulessa, G. S. Woods, and A. J. Clark

Title: A Theoretical Path Design For Long Range Over Ocean Microwave

Source: Proceedings of the IEEE Oceans Conference, Sydney Australia, May 2010, pgs. 1-4.

Summary: This paper reviews research on propagation in the maritime evaporative duct and then develops theoretical microwave path design. The theoretical results are compare with experimental results. The authors chose a model design height of 20 meters, anticipating a 20 meter or higher duct would be present 50% of the time. They also chose a frequency range of between 5 and 11 GHz, with 8 GHz being an optimum theoretical frequency that maximizes performance (minimum path loss). The actual data was the data from Article Number 2 above. It used 10.6 GHz with an antenna height of approximately 6 meters.

FDOT Project Relevance: The design in the paper will be considered as a reference for the design in this project.

Article Number: 5

Author(s): Kenneth Anderson, and Stephen Doss-Hammel

Title: Microwave and Infrared Propagation Over The Sea During The Rough Evaporation Duct (RED) Experiment

Source: Proceedings of the IEEE Military Communications Conference, Boston, October 2003, pgs. 1416-1421.

Summary: This paper describes the experimental results of a study in August-September 2001 off the coast of Hawaii that validated the evaporative duct propagation model in the US Navy's Advanced Refractive Effects Prediction System under rough sea conditions. The sea conditions for the experiments were wave heights of up to 2.5 meters and wave ages of 1 (ratio of wave velocity to wind velocity) under light wind conditions. The propagation parameters were 3 GHz (S band), 9.7 GHz (X band), and 17.7 GHz (Ku band) at two installed heights of 13 meters and 5 meters. The path link was approximately 390 km. At S band the higher height produced slightly better performance than the lower height. While for X and Ku band, the lower height performed better. At X band, there was ~ 30 dB range between the maximum and minimum path loss values but the standard deviation was 3-4 dB.

FDOT Project Relevance: The experimental design in the paper will be considered as a reference for the design in this project. In addition, the results will be compared with experimental data in this project.

Article Number: 6

Author(s): J. Ross Rottier, John R. Rowland, Gerald C. Konstanzer, Julius Goldhirsh, and G. David, Dockery

Title: APL Environmental Assessment for Navy Anti-Air Warfare

Source: Johns Hopkins Applied Physics Laboratory Technical Digest, Volume 22, Number 4, 2001, pgs 447-461.

Summary: This is a summary document that presents an overview of the Navy's need to understand atmospheric refraction and its impact on naval radar and communications. It begins with a technical discussion on atmospheric refraction and then presents the history of navy research, through the APL, on understanding atmospheric refraction and its effects on microwave propagation in the evaporative duct.

FDOT Project Relevance: Provides excellent background information on evaporative duct research from the 1980's up until 2001.

Article Number: 7

Author(s): V. Gadwal and A. Barrios

Title: Channel Modeling Using the Parabolic Equation for RF Communications

Source: Proceedings of the IEEE Military Communications Conference, Boston, October 2009, pgs. 456-461.

Summary: This is a report from the Space and Naval Warfare Systems Center Pacific, Atmospheric Propagation Branch, that introduces a wireless communications (and radar) channel model to help describe the non-linear time delay (and potential intersymbol interference) in atmospheric channels and especially surface ducts (which include the evaporative duct). The results suggest that communication channels operating in surface ducts with low-elevation transmitters and receivers experience shorter multi-path delays and therefore less intersymbol interference.

FDOT Project Relevance: This article provides background for understanding the expected dynamic channel conditions that will be experienced when the project is implemented.

Article Number: 8

Author(s): Shi Yang, Yang Kunde, Yang Yixin, and MA Yuanliang

Title: A New Evaporation Duct Climatology over the South China Sea

Source: Journal Of Meteorological Research, Volume 29, Issue 5, October 2015, pgs 764-778.

Summary: This is a report on the use of an improved evaporation duct model that incorporates more accurate stability functions. Using Frederickson's 2012 work (see Article 9 below), the authors work with the Navy Atmospheric Vertical Surface Layer (NAVSLaM) model, which was formerly the Naval Postgraduate School (NPS) model, and incorporate the atmospheric stability functions of Cheng and of Grachev. The results suggest that in northern subtropical regions of the study area, between about 17 and 23 degrees latitude (Key West is at 24.5 degrees latitude), the height of the evaporative duct ranges from 10-12 meters in January to August, 14 meters in September to November, and then 10 meters in December. The standard deviation of the duct height is highest in November at 2.5 meters. In the southern subtropical regions of the study area, between about 2 and 10 degrees latitude, the height of the evaporative duct ranges from a high of about 12 meters in September to a low of 9.6 meters in March. The standard deviation peaks at 2 meters in this region.

FDOT Project Relevance: This article, combined with the others in the literature search will help determine the expected evaporative duct height in the Gulf of Mexico.

Article Number: 9

Author(s): P. A. Frederickson

Title: Improving the Characterization of the Environment for AREPS Electromagnetic Performance Predictions

Source: Weather Impacts Decision Aids Workshop, Reno, NV, March 15, 2012, pgs 6-8, and Microsoft Powerpoint presentation from the Desert Research Institute, available on the internet at:http://www.dri.edu/images/stories/conferences_and_workshops/wida/presentations/Frederickson_WIDA_2012_Brief_-_15_Mar_2012.pptx , *accessed May 29, 2016.*

Summary: This is a presentation on the current state of research at the Naval Postgraduate School that is being conducted to improve the Advanced Refractive Effects Prediction System

(AREPS) electromagnetic propagation model. The presentation focuses on recent improvements made in resolution, stability, and in accuracy.

FDOT Project Relevance: During the project if access to AREPS is permitted, then the model will be used to help predict propagation conditions in the Gulf of Mexico.

Article Number: 10

Author(s): W. L. Patterson

Title: Advanced Refractive Effects Prediction System (AREPS)

Source: Proceedings of the IEEE Radar Conference, Boston, April 2007, pgs 891-895.

Summary: This article describes the Advanced Propagation Model (APM) and its graphical user interface, AREPS. Both APM and AREPS are accredited within the Navy Modeling and Simulation Office. AREPS is also a North Atlantic Treaty Organization (NATO) simulation application. These tools are used to predict propagation conditions over land and sea paths and during varying climate conditions. They are used for research and for tactical purposes. They have been used extensively in the research on microwave propagation through evaporative ducts and represent the state of the art in this field.

FDOT Project Relevance: During the project if access to AREPS is permitted, then the model will be used to help predict propagation conditions in the Gulf of Mexico.

Article Number: 11

Author(s): Michael J. Luddy, Jack H. Winters, and Alex Lackpour

Title: Beyond Line-of-Sight Communications with Smart Antennas

Source: Proceedings of the American Society of Naval engineers, Intelligent Ships Symposium IX, Philadelphia, May 2011, pgs 891-895.

Summary: This article describes the use of adaptive antenna systems and communication techniques that use Multiple Input Multiple Output (MIMO) techniques and Orthogonal Frequency Division Multiplexing (OFDM) to mitigate and exploit the multipath and delay spread impairments associated with beyond line of site communications in a surface duct by naval surface and airborne assets.

FDOT Project Relevance: If this project is a success, potential follow on work will take advantage of this research. Toward that end, if time permits it may be possible to investigate OFDM as a signal transmission technique that can improve performance in this project.

Article Number: 12

Author(s): H. J. Hansen, A. S. Kulessa, W. Marwood, M. Forrest, D. Borg, and O. Reinhold

Title: Multipath and anomalous propagation studies of Ka band emissions using a distributed transmit-receive radio link network experiment

Source: Proceedings of the Asia-Pacific Microwave Conference, Melbourne, December 2011, pgs 749-752.

Summary: This article describes experimental results for a surface duct propagation study at millimeter wave frequencies. The experimentation was conducted over a 11 kilometer link over water along the coast of a small bay in southern Australia (33 degrees south latitude) in November.

FDOT Project Relevance: Despite using different frequencies, a shorter path, and different environmental conditions (small bay verses a gulf), this article does contribute some assistance in experimental set-up that can be adapted to the FDOT project.

## CHAPTER 3. DESIGN

The microwave propagation project will use a transmitter station located at Key West, Florida, and a receiver station located at Destin, Florida. Both stations will be installed on trailers owned by the Florida Department of Transportation (FDOT). Each trailer will also be supported by a second trailer that is configured as a power plant that will harvest solar power to be used to power the microwave propagation stations.

The microwave transmitter and receiver stations will use Software Defined Radios (SDR) to create and receive the test signal. A small computer will be used to control the SDRs at each end. The software that will be used is Mathworks Matlab and Simulink running under Windows 7 on the small computer. The SDRs and small computers, along with the software will be loaned to the project by UNF. A cellular modem will allow the University of North Florida (UNF) to remotely run the propagation tests. Using the modem and remotely accessing the small computer, UNF research staff, working from the UNF campus in Jacksonville, Florida, will configure the transmitter in Key West and initiate a test transmission. At the same, the UNF researchers will also access the small computer in Destin and initiate a test reception.

The transmitter is designed as a double conversion RF transmitter. Under the control of the small computer, the SDR will transmit a 270-megahertz (MHz) signal along an RF cable up the trailer tower to a large 2.4-meter antenna. Behind the antenna, in an outdoor equipment enclosure, the transmitter will convert the 270-MHz test signal to a 1,020-MHz intermediate frequency (IF) test signal, and then convert the 1,020-MHz IF to one of two final RF frequencies, either 5,840 MHz or 10,250 MHz. These two frequencies were chosen because they are available for testing and are close to commercial frequencies that a permanent system would use if the tests are successful. The frequency up-conversions will be accomplished using connectorized microwave components. Some of these components, including frequency mixers, amplifiers, and attenuators, are off-the-shelf components. The final power amplifiers that operate at 5,840 MHz and 10,250 MHz are expensive and exceed $1,000 each which requires then to be procured as equipment.

In addition to off-the-shelf components, the transmitter and receiver include custom filters and also custom phase-locked loop oscillators that provide very stable references for the test frequencies to be generated. The oscillators use an external reference of 10 MHz that is provided by a Global Positioning Satellite (GPS) disciplined oscillator reference. This also reduces the concern about operating the oscillators in the higher temperature environment of an outdoor antenna-mounted enclosure. The GPS reference is located at the base of the tower with the software-defined radio and the small computer. There are three pairs of oscillators (the same three oscillators are used at the receiver), and they are procured as equipment due to their expense.

The antenna system at both the transmitter and the receiver site includes a large antenna and the motors to permit the antenna to be turned remotely. This feature allows the antenna positions to be adjusted as part of the testing procedures. The controller needed to precisely control the motors and therefore accurately position the antennas is procured as equipment due to its expense.

The transmitter site also includes a power sensor for monitoring the output power (forward and reflected) to ensure that the transmitter site is actually transmitting energy. This avoids the possibly of concluding a signal cannot be propagated when in fact the transmitter had failed. The power sensor is sophisticated and procured as equipment due to its expense.

The receiver site looks like the mirror image of the transmitter site. However, there are no final power amplifiers and no power sensor. Instead, the receiver antenna system is attached to two high performance low-noise amplifiers that are procured as equipment. After these amplifiers, the received signal is frequency down-converted twice using the same frequencies and equipment configurations as the transmitter. A 270 MHz received signal is sent down the tower to the receive SDR and small computer where tests can be monitored remotely from Jacksonville using a cellular modem.

The power systems for the two microwave propagation stations are slightly different. The receiver site will consume approximately 118 Watts when operational. A 1,000 watt solar power plant will provide enough power to run this receiver site. The project will install the power plant on a trailer on loan from the FDOT for the project. The transmitter will consume approximately 165 Watts when operational. A second 1,000 Watt solar power plant will assist in providing power to the transmitter site trailer. The FDOT trailer that is planned for the transmitter site has 400 Watts of solar power onboard already and the 1,000 Watts will augment the 400 Watts to provide enough power to run the transmitter site. The FDOT has enough battery power storage available to store the required energy for use between daytime charging periods. Heavy gauge 2/0 cables will be used to connect the power plant trailers to the microwave test trailers. The desired voltage output from the solar power system is 24 Volts (V) Direct Current (DC). Voltage converters that convert DC to DC will be used to provide other voltages including 5 V, 12 V, and 15V.

The drawings for the design are presented in Appendix 1. There are three drawings for the transmitter site and three drawings for the receiver site. The component numbers on the drawings can be found on the procurement order sheets in Appendix 2. This is used to assist in identifying which vendor’s part is needed for each design component.

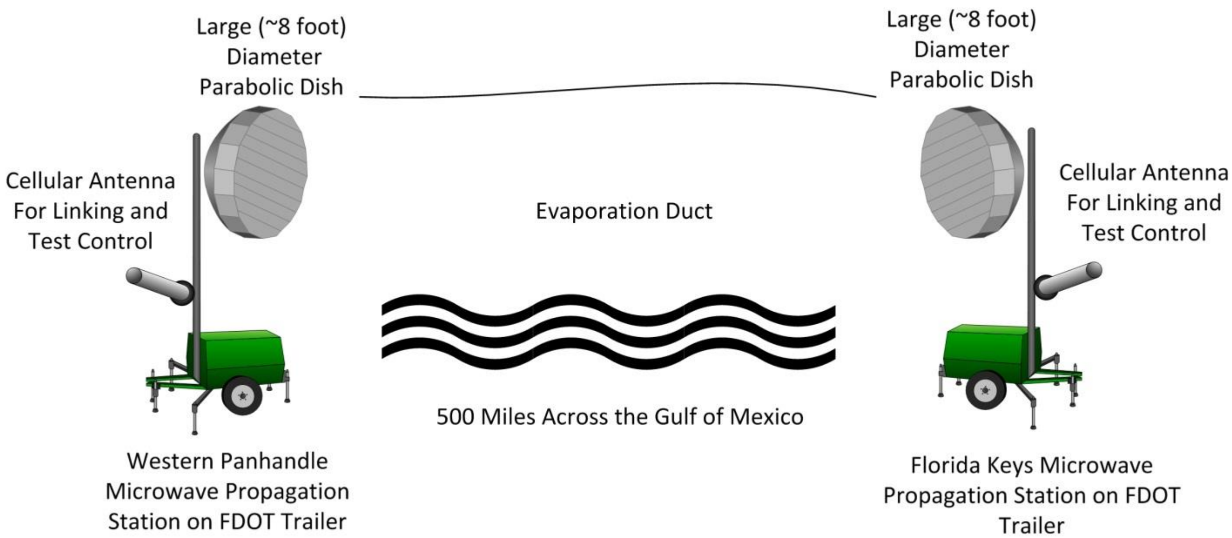


Figure 1. Microwave test stations on deployment.

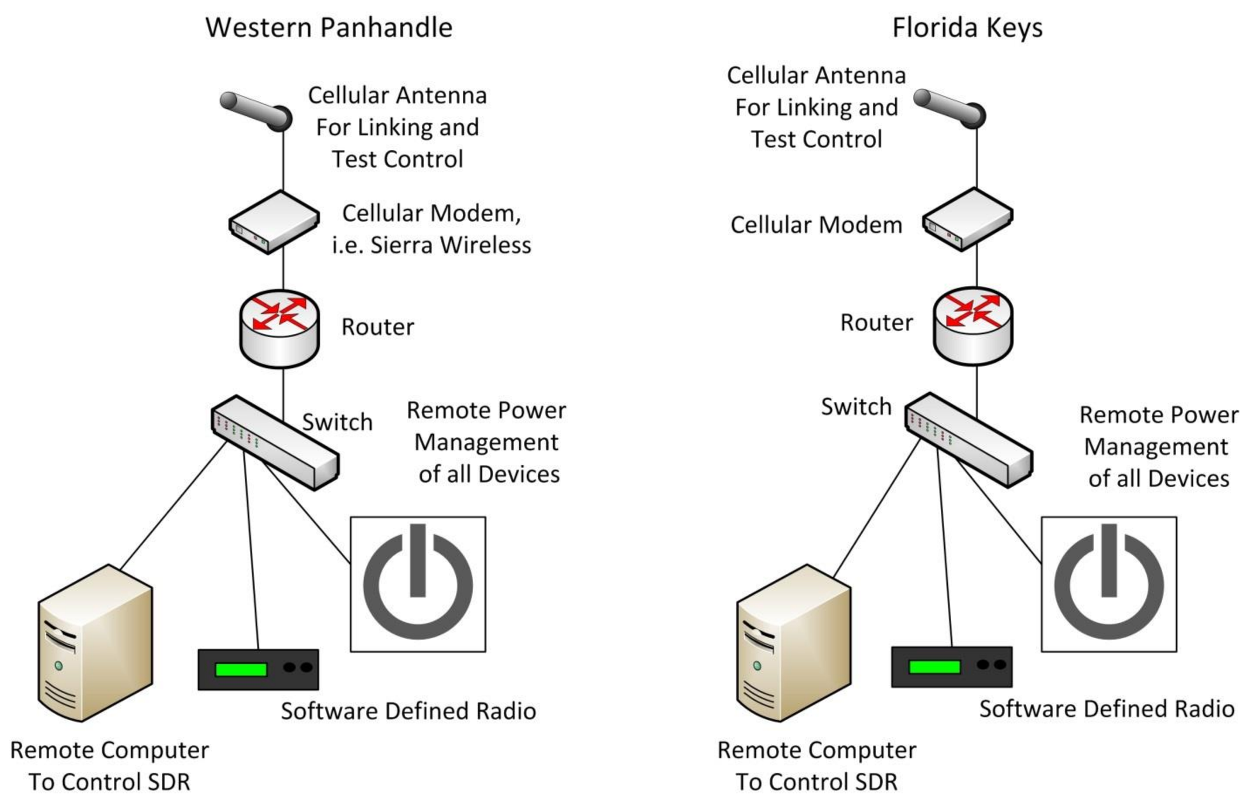


Figure 2. Command, Control and Communications (C3) layout.

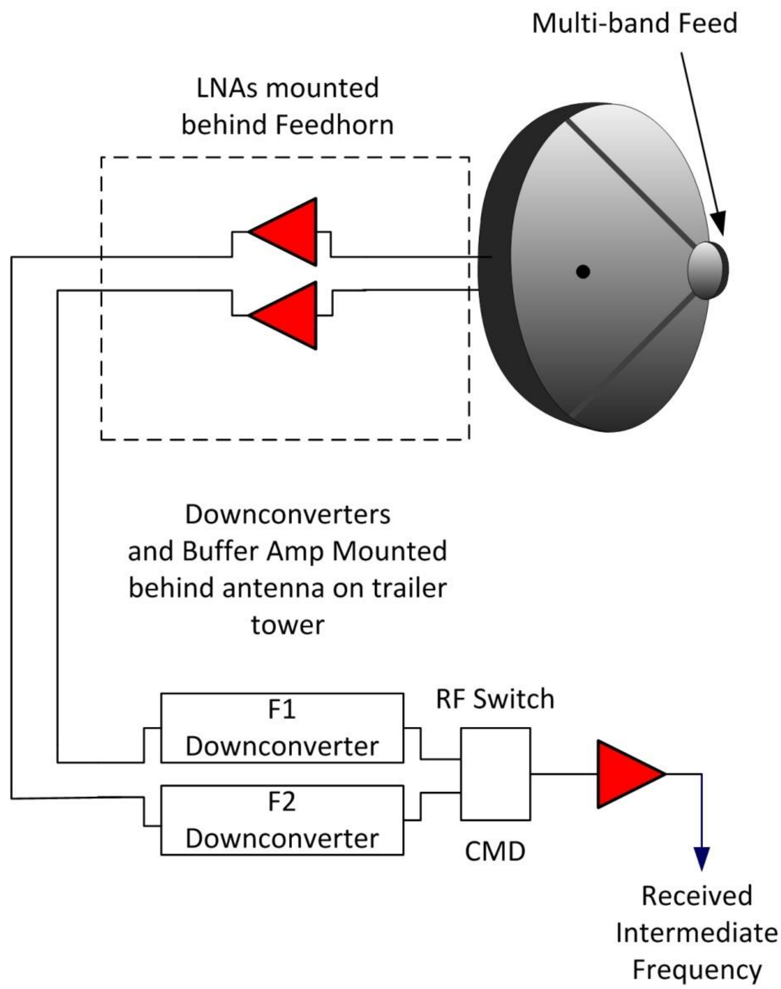


Figure 3. Receiver microwave test station design.

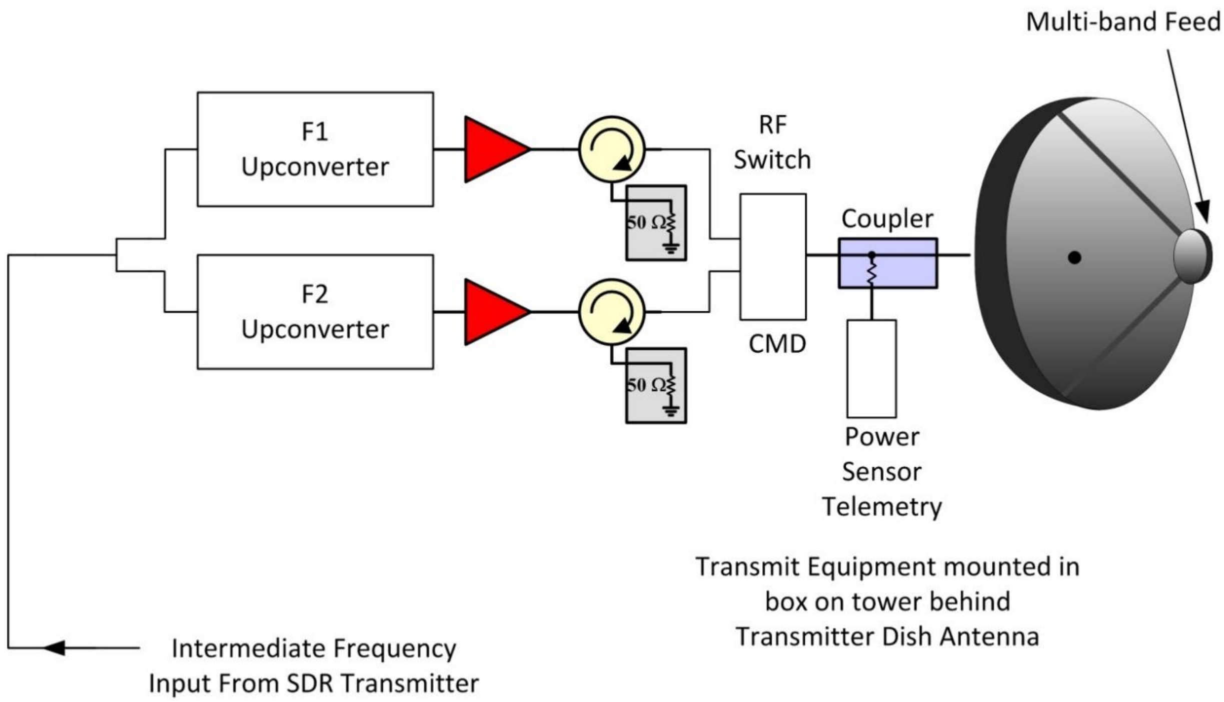


Figure 4. Transmitter microwave test station design.

# CHAPTER 4. PROCUREMENT

This project required a significant amount of equipment and materials. The logistics of the procurement of these devices was important enough that a task was identified that would focus entirely on acquiring them. An initial concern was that if the desired equipment could not be procured, the entire design would need to change, precipitating a domino effect that might mean other previously secured devices would no longer be appropriate. Significant effort was applied to ensure that equipment and materials that are readily available were planned for use in the project. Despite this effort, University of North Florida internal procurement policy issues, unknown to the research team, caused the project to abandon a preferred vendor of the most expensive equipment item in the project, in favor of a secondary vendor. Since two quotes for the equipment device had been secured, the change of vendors only affected internal project costs. The overall cost of equipment remained within budget and only a minor design change was necessary.

The procurement process was completed successfully. There was sufficient funding for the entire procurement, and funding reserves remained for use during the project in the event minor anomalies occurred with the equipment or materials. The logistical effort to procure over 50 items for the project required product research, cost estimating, and vendor discussions. The initial effort was an iterative process, interwoven with the design process. As design criteria were developed, available equipment and materials were considered. Depending on availability, the design criteria were maintained or changed to adjust to what could be procured cost effectively and in a timely manner. The equipment is shown in Table 1, and the materials are shown in Table 2.

There was one issue with the procurement process that may suggest the FDOT Research Center should clarify its policies regarding the purchase of equipment and materials. The agreement between the FDOT and UNF indicates that federal procurement rules are to be used. However, during the procurement process, UNF decided that state procurement rules, which were more restrictive, must be followed. This prevented the use of a lowest-price federally approved vendor (Nexyn). To resolve the matter, the FDOT Research Center permitted UNF to use the second choice, more expensive vendor (Wenzel Associates). If the FDOT Research Center supports this application of state procurement rules they may want to clarify in the standard terms and conditions of a research agreement that state procurement rules are also to be followed in executing these federally funded research agreements.

Table 1. Project Equipment Items

| Item | Description | Invoice Amount | Serial Number (s) |
|---|---|---|---|
| 1 | 2 GPS Disciplined Oscillators, Trimble Thunderbolt 60333-50, Vendor is Novotech | $1,393.20 + $80 shipping | 51040759<br>51040787 |
| 2 | 6 Phase Lock Loop Oscillators, Wenzel Associates, Part Numbers:<br>500-29611, Quantity 2<br><br>500-29612, Quantity 2<br><br>500-29608, Quantity 2<br><br>Wenzel was not the low bidder. (See narrative) | <br><br>$9,224.00<br><br>$10,920.00<br><br>$7,240.00 | <br><br>25334B001<br>25334B002<br>25334C001<br>25334C002<br>25334A001<br>25334A002 |
| 3 | 2 X-Band Filters, Reactel 4C3-10250-X200S11 | $808.00 + $17 shipping | 16-01<br>16-02 |
| 4 | 2 Power Amplifiers, Advanced Microwave, Quantity 2 Part Numbers<br>PA2403P<br>PA2803P | <br>$3,350.00<br>$3,940.00 + $36 shipping | <br>1001<br>1104 |
| 5 | 1 Intelligent Power Sensor, Ladybug LB5912A | $2,412.00 + $15 shipping | 157180 |
| 6 | 2 Low Noise Amplifiers, RF Lambda, Part Numbers<br>RLNA09G10G<br>RLNA04G08G | <br>$1,350.00<br>$1,350.00 + $125 shipping | <br>15040600367<br>16092600183 |
| 7 | 2, 8-Foot Parabolic Antenna Systems: Spid Elektronik MD-02 controllers and RAS/HR antenna motors. Vendor is RF Ham Design. Serial Numbers are on the MD-02 controllers. | $3,664.00 + $431 shipping + 3.9% bank charge $142.90 | 70368<br>70373 |
| | **EQUIPMENT TOTAL** | **$46,498.10** | |

Table 2. Project material vendors.

| Number | Vendor | Material Procured |
|---|---|---|
| 1 | Advantech B&B SmartWorx | USB over Ethernet servers and Ethernet Switches |
| 2 | Del City | Solar Power Cables and Hardware |
| 3 | EcoDirect | Hyundai Solar Panels and Outback Solar Chargers |
| 4 | Fairview Microwave | RF Circulators |
| 5 | Industrial Networking Solutions | Cellular Modems and Antennas |
| 6 | LanShack | Fiberoptic Cables |
| 7 | L-Com | Outdoor Equipment Enclosures |
| 8 | Mini-Circuits | RF Mixers, amplifiers, attenuators, splitters, switches, terminations, diplexers |
| 9 | Mouser | Power Supplies |
| 10 | NexTek | RF Lightning Protectors |
| 11 | Novotech | GPS Receivers and 10 MHz GPS-Disciplined Oscillators |
| 12 | Pasternack | RF Directional Couplers |
| 13 | Reactel | RF Filters |
| 14 | Tessco | RF and DC Lightning Protectors, Ground Bars, RF Adapters |
| 15 | Wenteq | RF Circulators |

## CHAPTER 5. CONSTRUCTION AND TESTING

The two test stations were each constructed by following the design approach presented in the task 2 report and outlined above in Chapter 3. The two test stations were constructed in parallel to ensure the layouts of both stations were similar. This similarity in the station layouts simplifies and accelerates testing, maintenance, and troubleshooting. The design as-built drawings describe the construction of the two test stations. These drawings are divided into three areas, control communications, Radio Frequency (RF) systems, and power.

The drawings that discuss the control communications of the two test stations are presented in Figures 5 to 7. The general schematic for control communications is presented in Figure 5. A specific plan for control communications of the transmitter test station is displayed in Figure 6 and for the receiver in Figure 7.

The RF systems make up the next group of design as-built drawings. Figures 8-10 show the RF systems of the transmitter test station. The receiver test station RF systems are displayed in Figures 11-13.

Power is the third area addressed by the design as-built drawings. Figure 14 shows the main power distribution panel schematic that is used by both the transmitter and receiver test stations. The power sub panel schematic for the transmitter test station is shown in Figure 15 and the power sub-panel for the receiver test station is shown in Figure 16. The final design as-built drawing shows the unique solar power plant that was developed for the receiver test station and is shown in Figure 17.

The testing of the test stations is a two-phase process. In the first phase of testing the subsystems of the test stations were tested. This involved testing each of the components of the subsystems to ensure the assembled stations would function correctly. In a second future testing phase the assembled test stations will be tested as a complete system. This task report addresses only the phase one subsystem testing.

The phase one testing of the subsystem components was conducted using test procedures that are presented in Appendix 1. The goal of each test procedure was to determine if each component of the subsystems was performing according to specifications. Sine the design was based on these specifications, this approach ensures that the constructed subsystems will function nominally. The tests required the use of specialized test equipment. This equipment used for the tests is presented in Table 3. All of the test equipment was new and/or recently calibrated to ensure accurate test results.

There are three categories of subsystem components that required testing. The three categories are amplifiers, RF filters and oscillators. The testing for amplifiers validated that the power amplification, at the desired operating frequency and desired input power level, was within specification. The testing of the RF filters required validating that the bandwidth and insertion loss was within specification. For the oscillators, the testing validated that the frequency and power level were within specification. The three tables below show the test result for the components of the subsystems. Table 4 shows the test results for amplifiers. Test results for RF filters and oscillators are shown in Tables 5 and 6 respectively. All subsystem components passed the required tests successfully.

It is anticipated that the subsystems will be integrated to their test stands during a future project and that final phase two testing will ensure that the integration was successful and that the test stands are operating nominally.

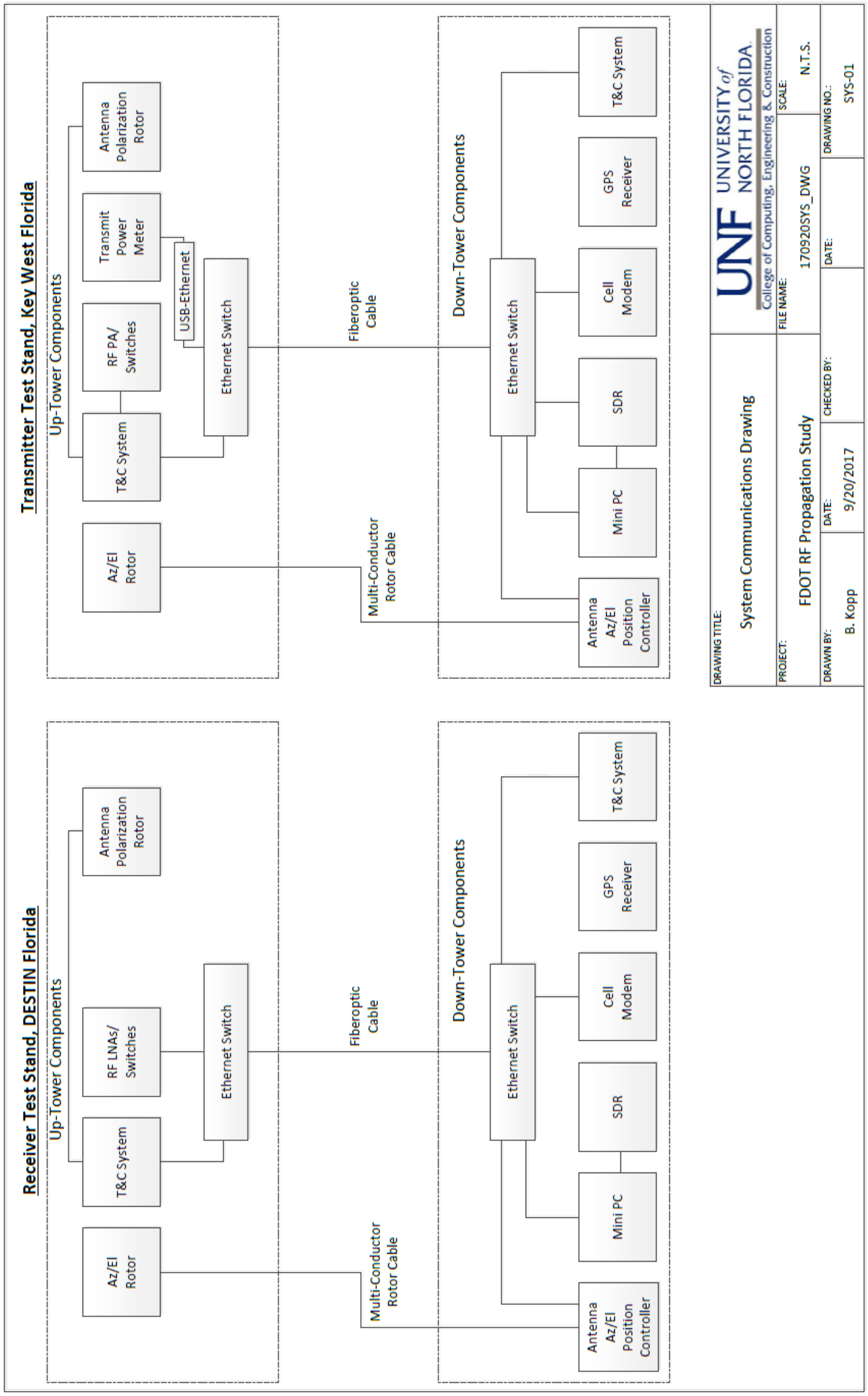


Figure 5. Test station control communications layout.

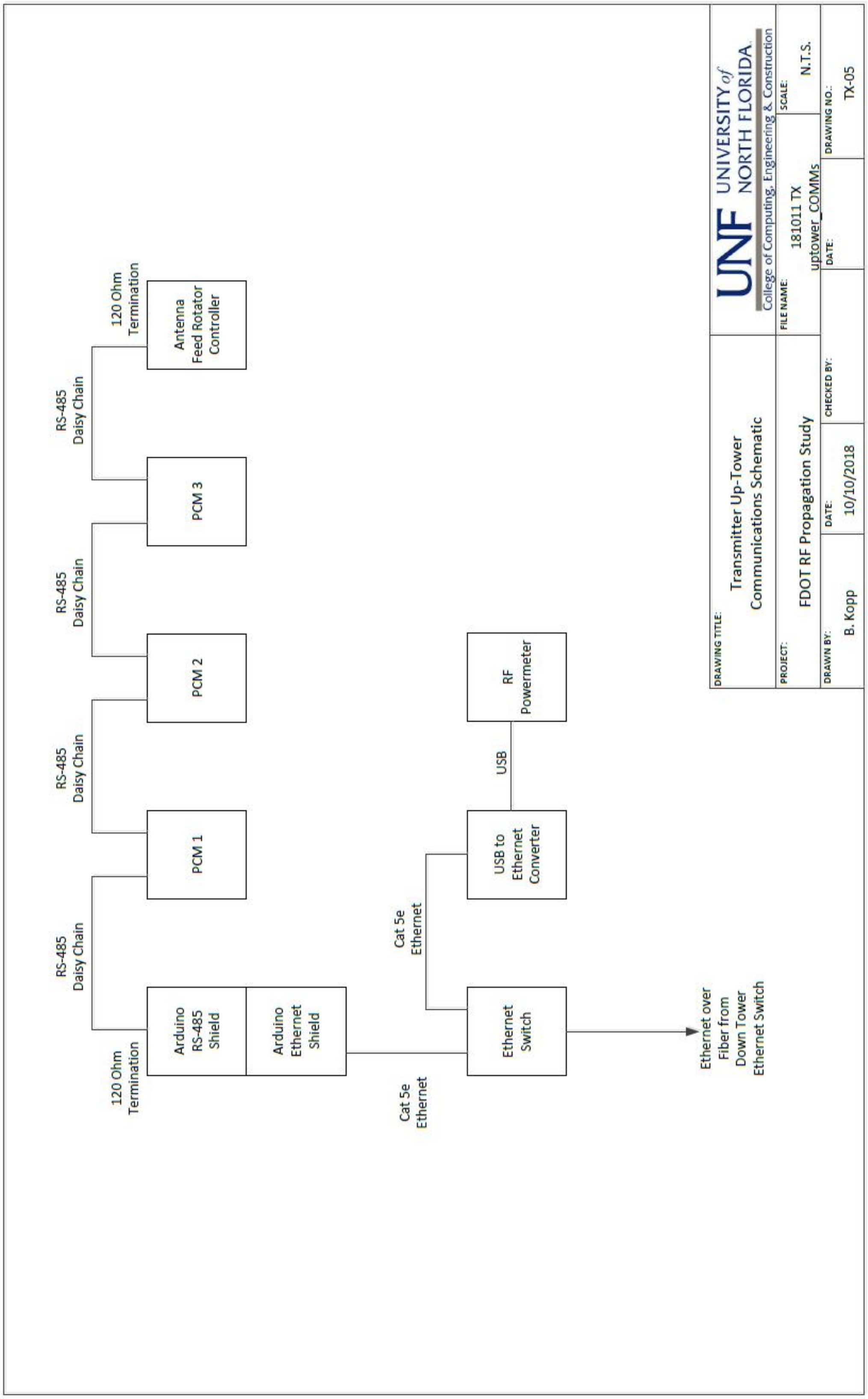


Figure 6. Transmitter test station control communications details.

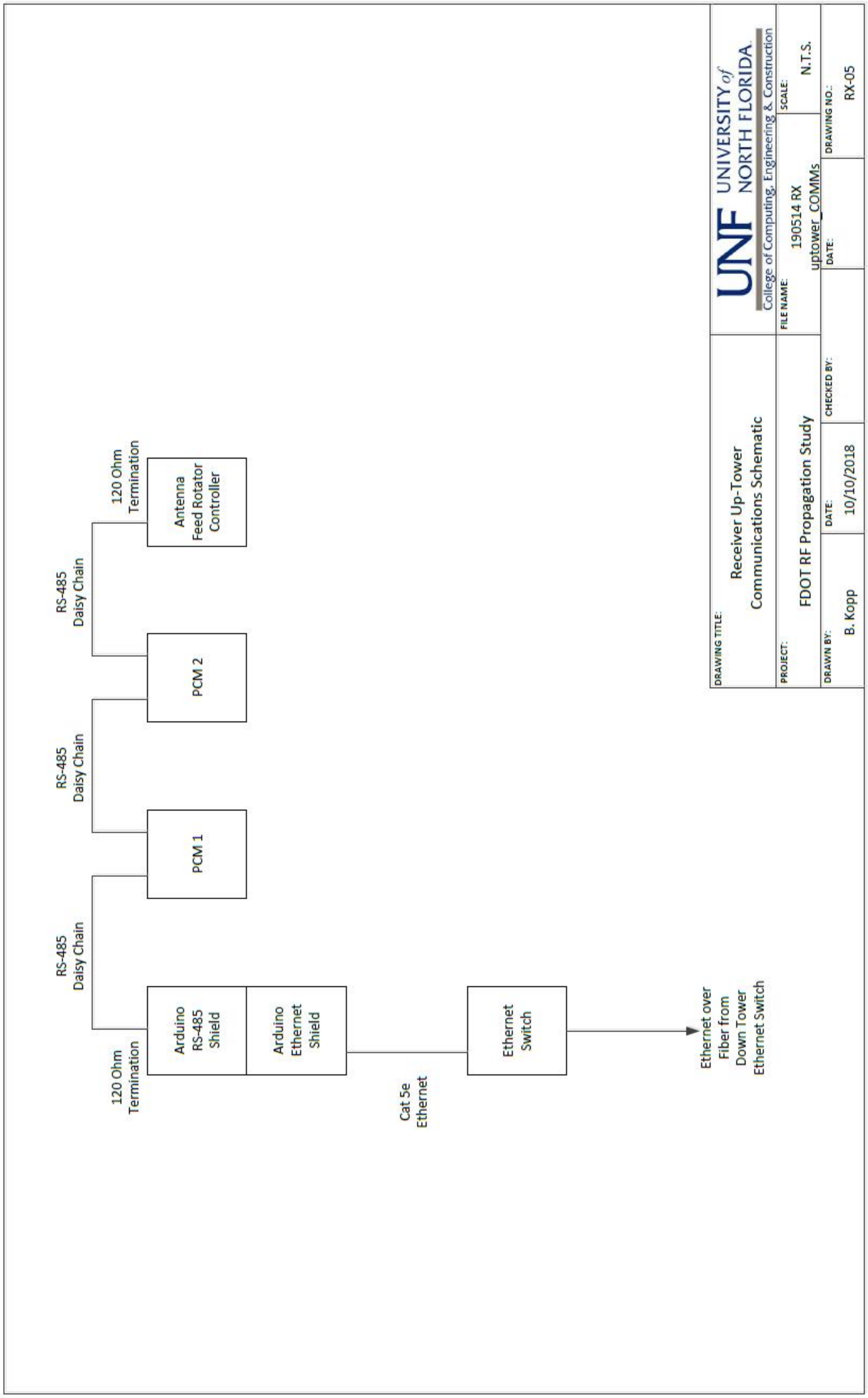


Figure 7. Receiver test station control communications details.

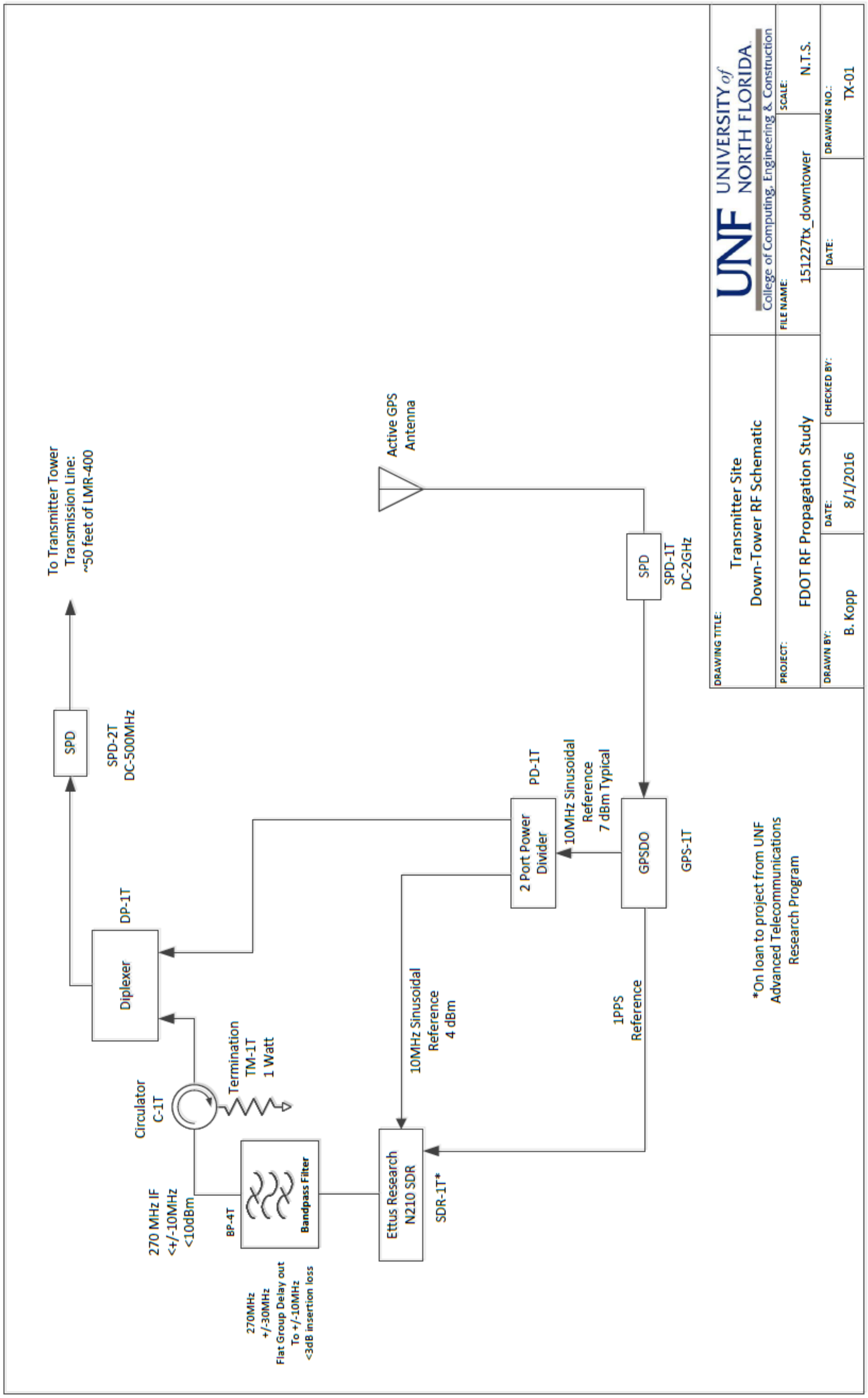


Figure 8. Transmitter test station RF system, part 1.

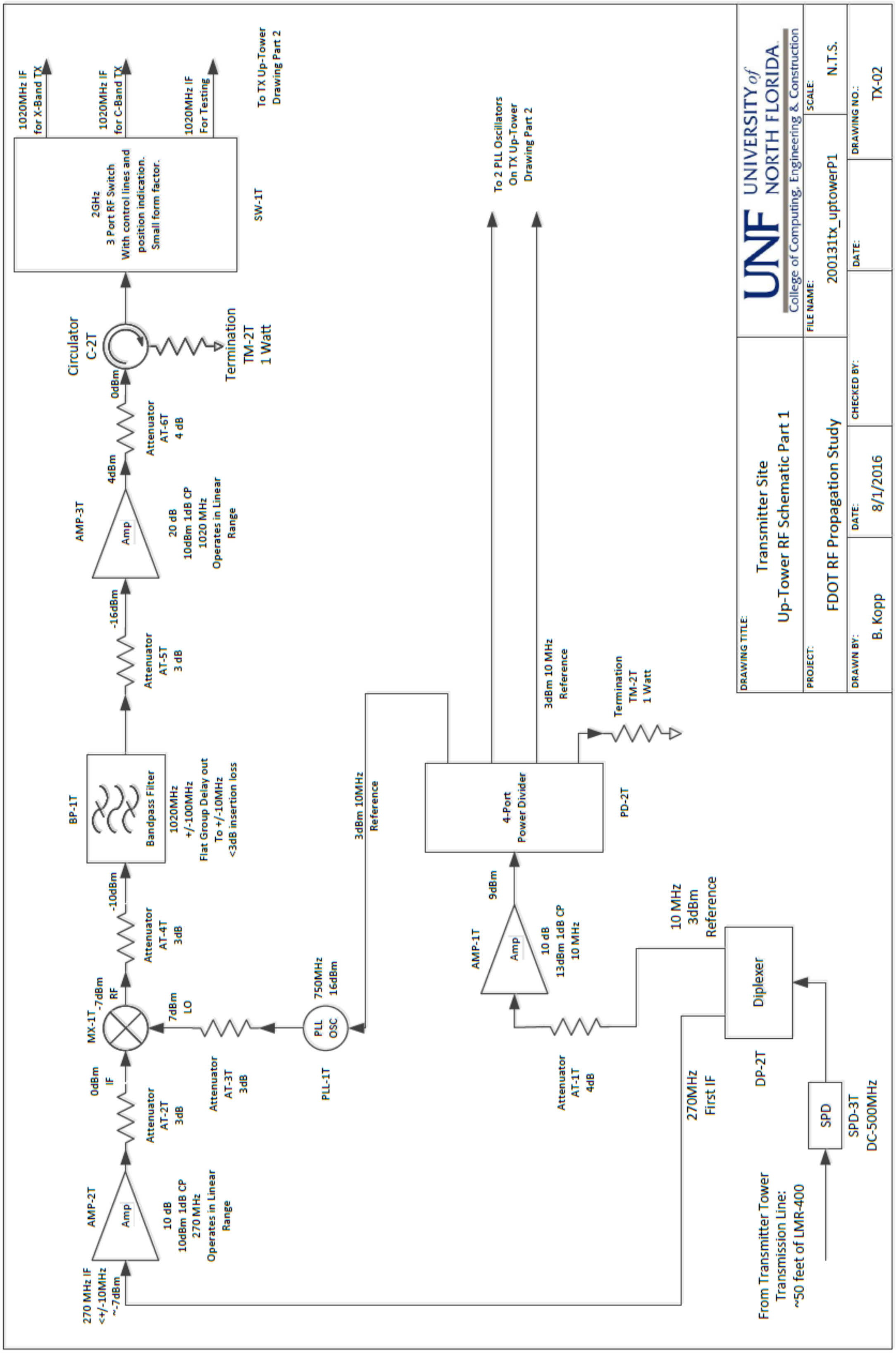


Figure 9. Transmitter test station RF system, part 2.

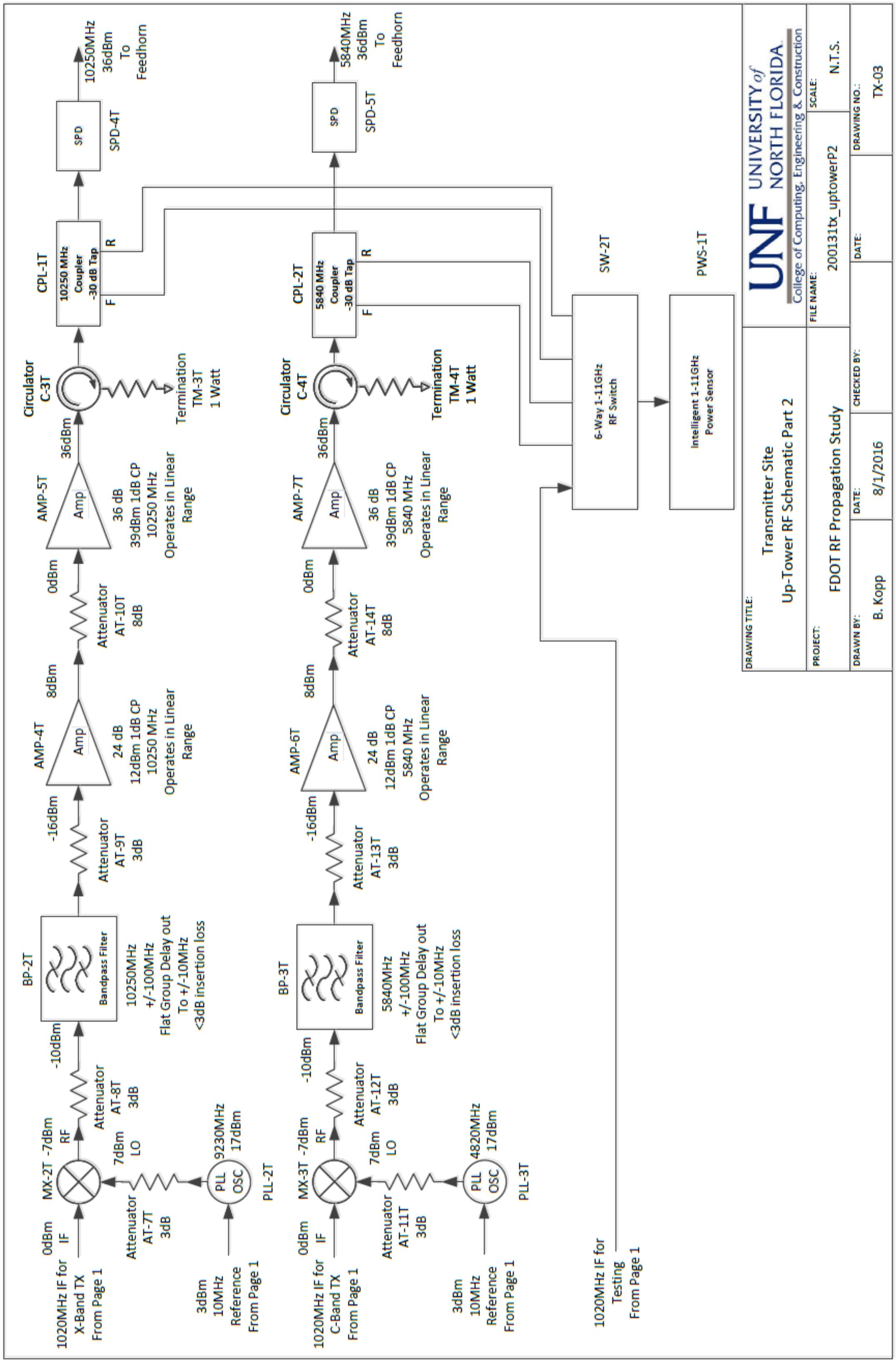


Figure 10. Transmitter test station RF system, part 3.

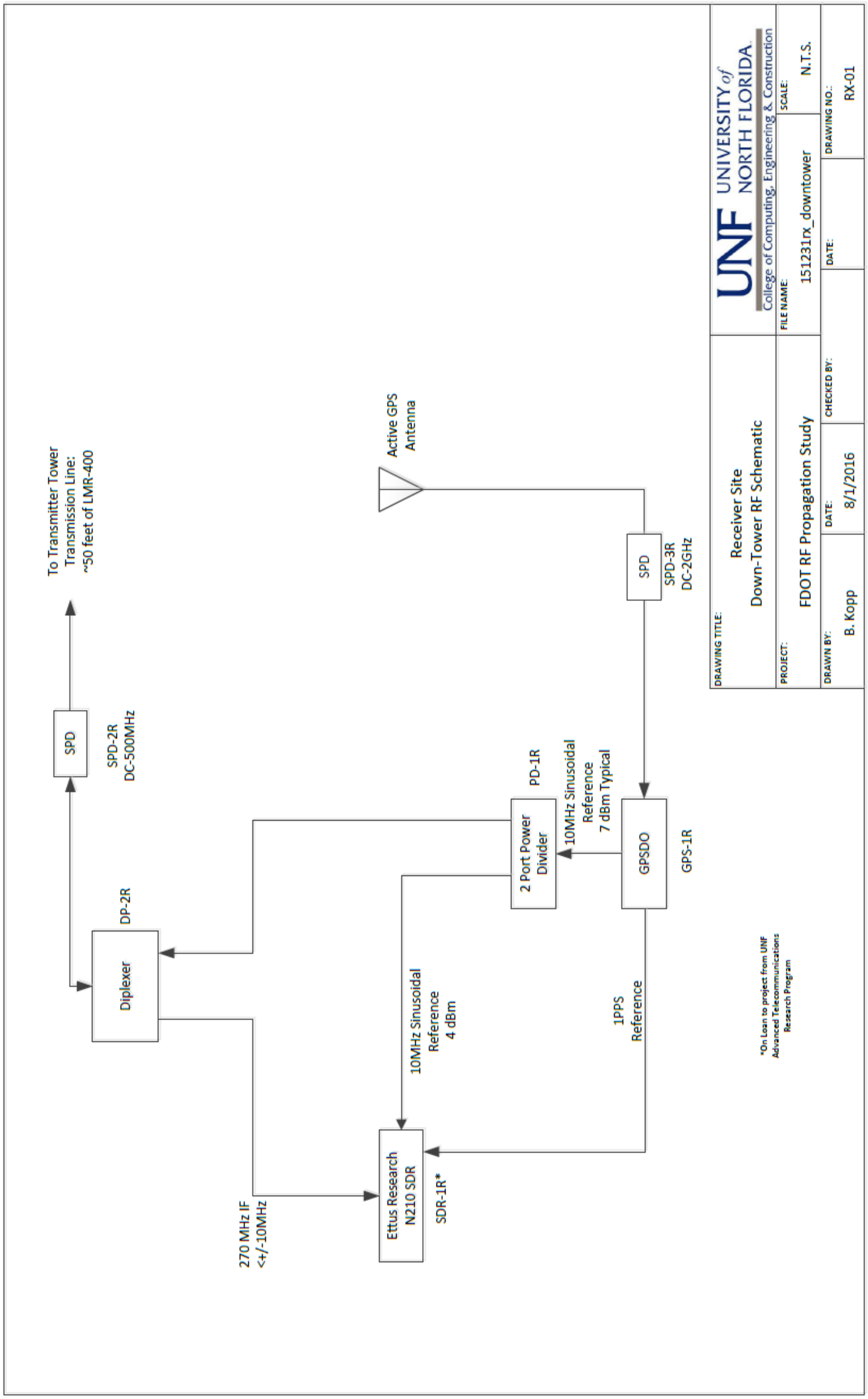


Figure 11. Receiver test station RF system, part 1.

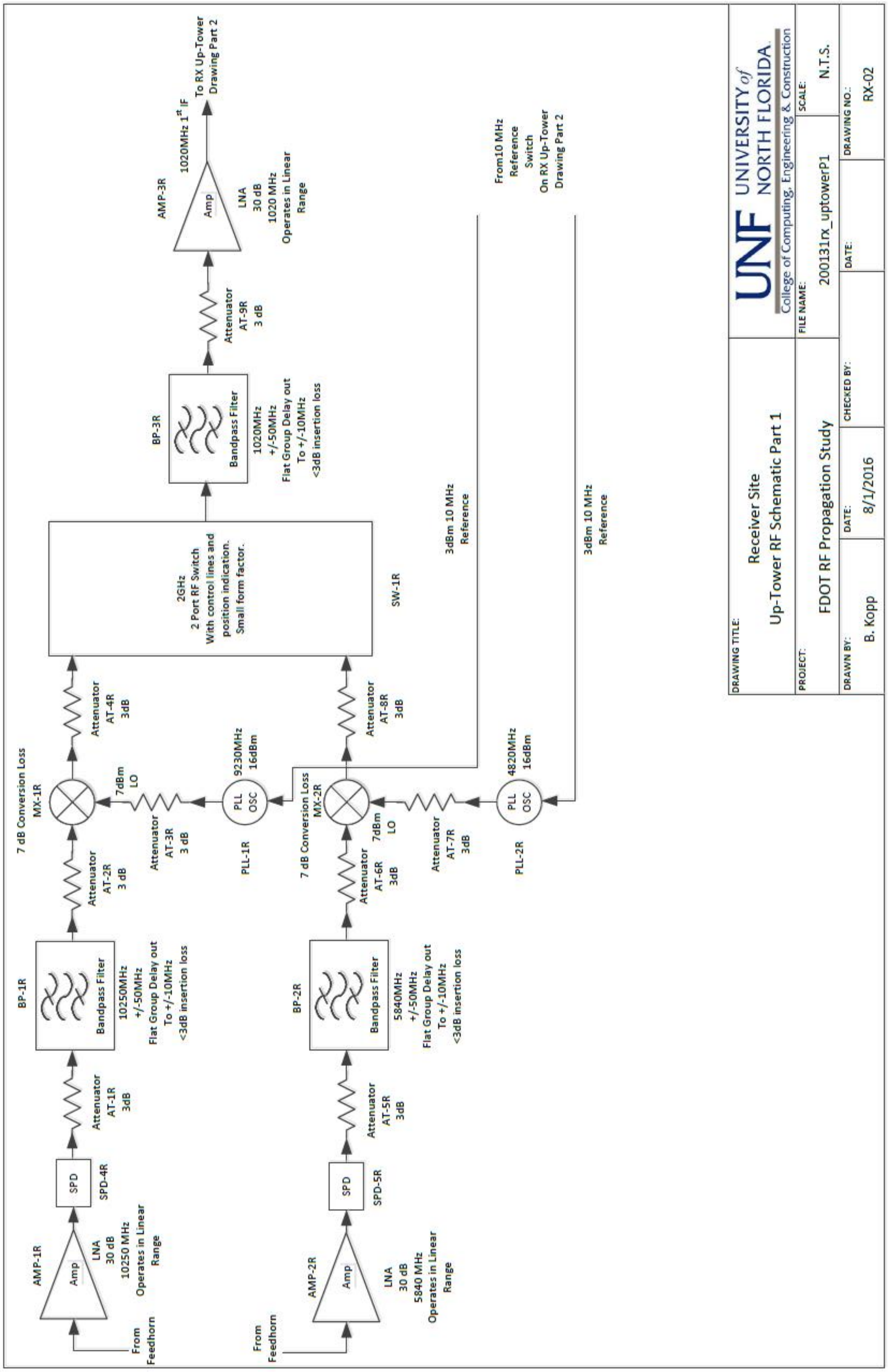


Figure 12. Receiver test station RF system, part 2.

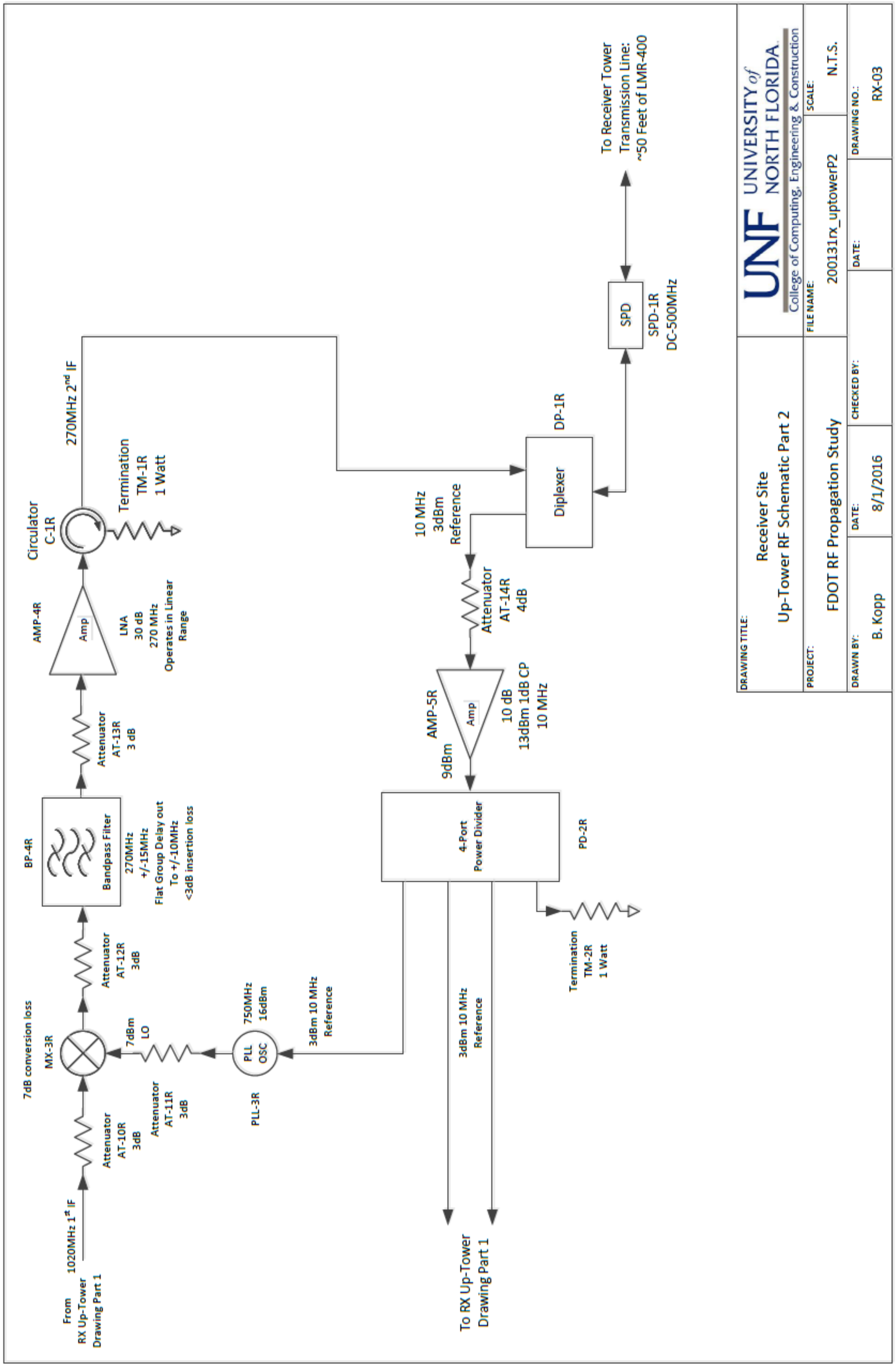


Figure 13. Receiver test station RF system, part 3.

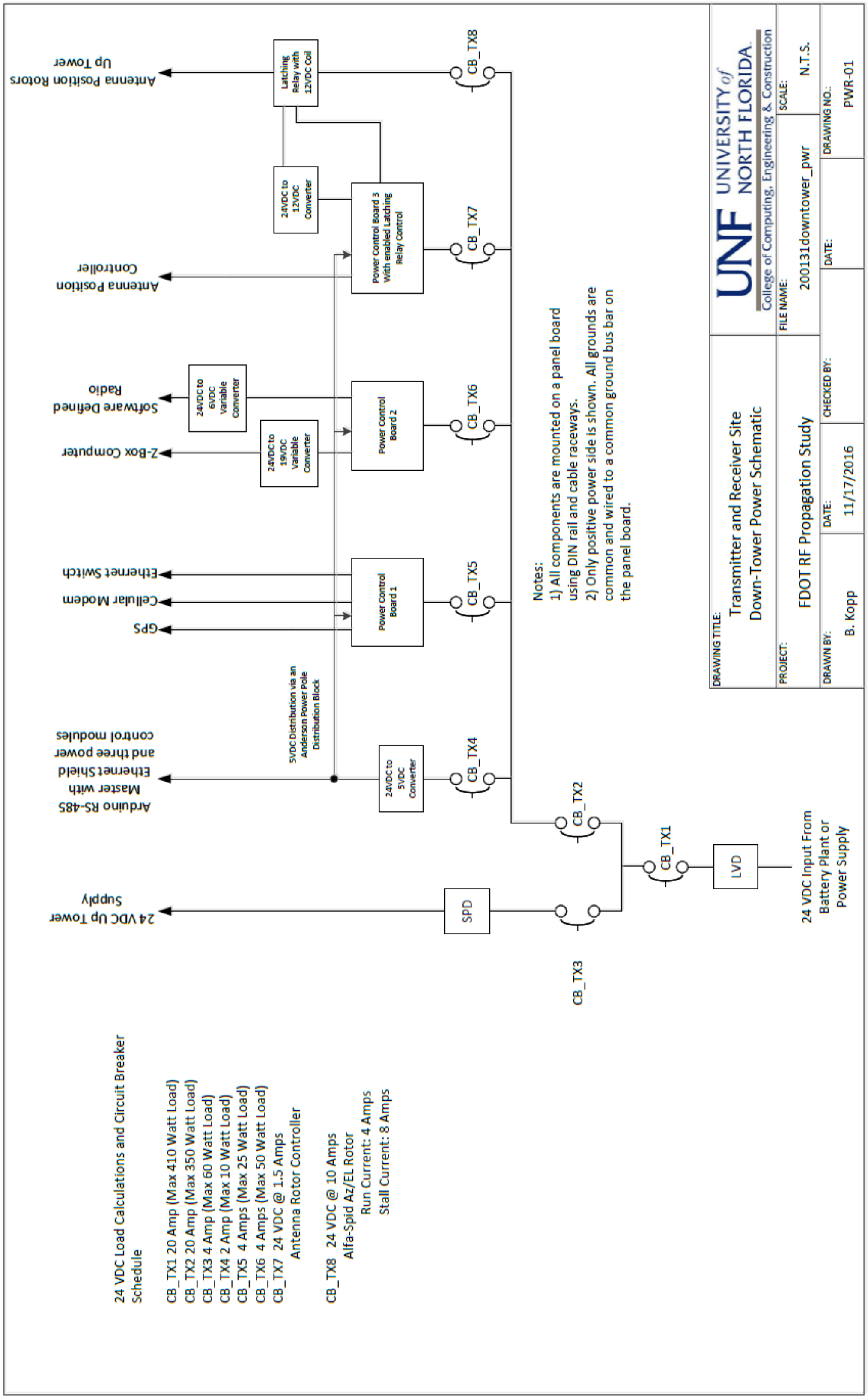


Figure 14. Main power distribution panel for both test stations.

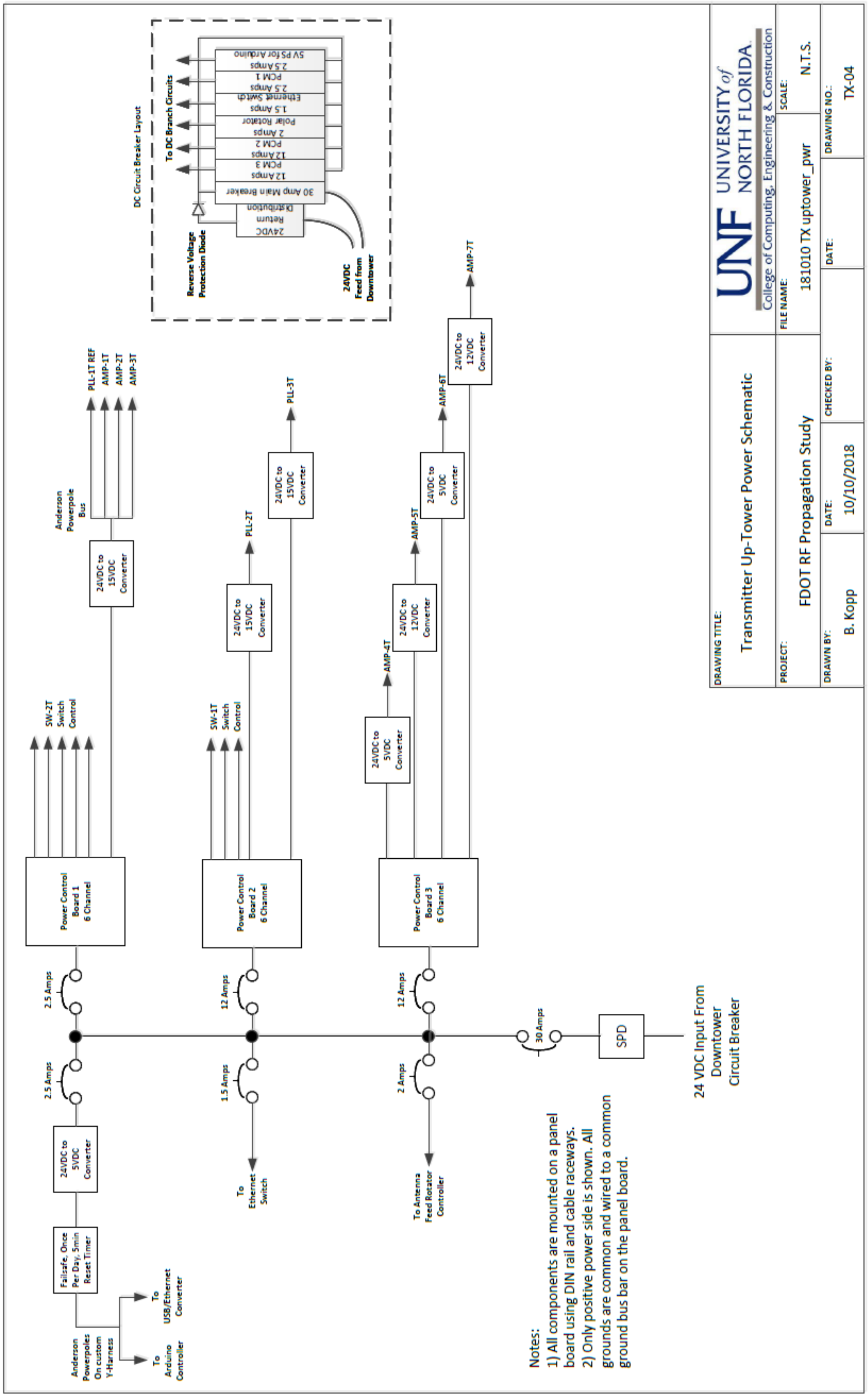


Figure 15. Transmitter sub-panel power distribution.

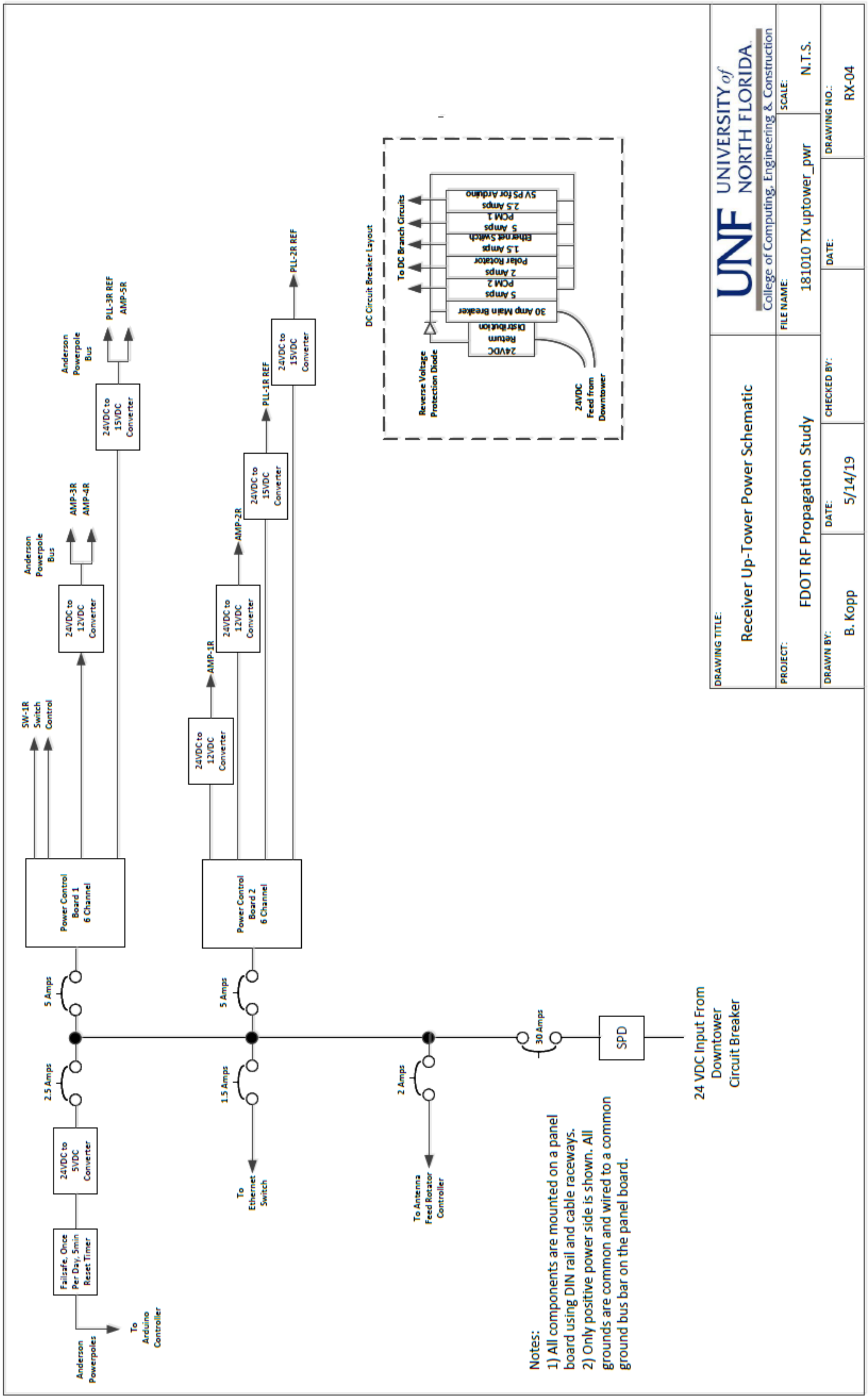


Figure 16. Receiver sub-panel power distribution.

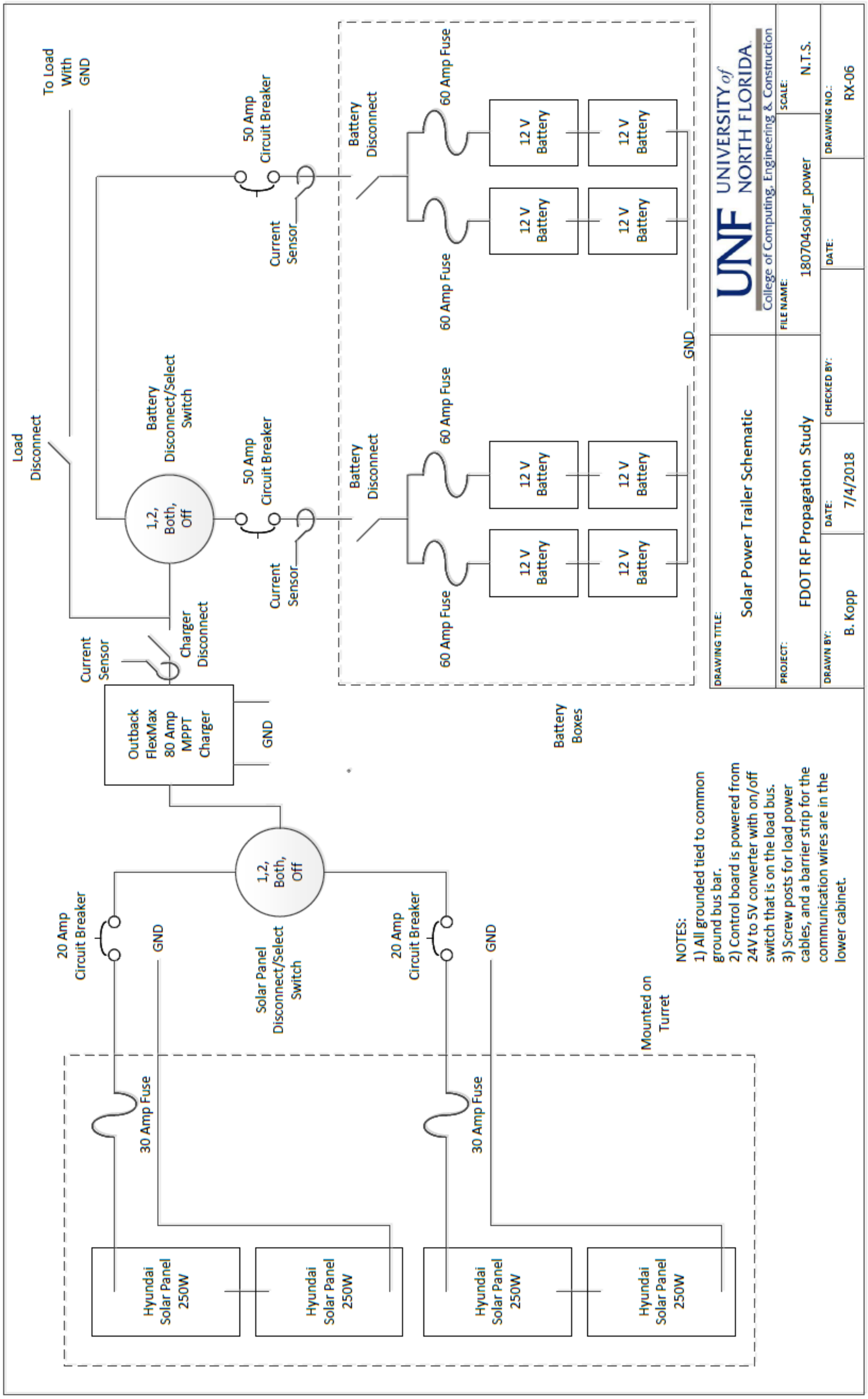


Figure 17. Receiver test station solar power plant design.

Table 3. Subsystem test equipment.

| Item | Description | Manufacturer | Part Number |
|---|---|---|---|
| 1 | Spectrum Analyzer | Signal Hound | USB-SA124B |
| 2 | Tracking Generator | Signal Hound | USB-TG124A |
| 3 | Signal Generator | Rigol | DSG3060 |
| 4 | DC Power Supply | Xantrex | HPD 60-5 |
| 5 | DC Power Supply | Xantrex | HPD 60-5 |
| 6 | Function/Arbitrary Waveform Generator | Rigol | DG4162 |
| 7 | Power Sensor | LadyBug Technologies | LB5912A |

Table 4. Amplifier test results.

| Item | Project Part Number | Manufacturer | Manufacturer Part Number | Spec. Amp. Gain | Subsystem Frequency | Subsystem Amplifier Input Level | Test Pass / Fail |
|---|---|---|---|---|---|---|---|
| 1 | AMP-1T | Mini-Circuits | ZFL-1HADB+ | 10 dB | 10 MHz | -1 dBm | Pass |
| 2 | AMP-2T | Mini-Circuits | ZFL-1HADB+ | 10 dB | 270 MHz | -7 dBm | Pass |
| 3 | AMP-3T | Mini-Circuits | ZFL-2000B+ | 20 dB | 1,020 MHz | -16 dBm | Pass |
| 4 | AMP-4T | Mini-Circuits | ZX60-24-S+ | 24 dB | 10,250 MHz | -16 dBm | Pass |
| 5 | AMP-5T | Adv. UWave | PA2803P | 35 dB | 10,250 MHz | 0 dBm | Pass |
| 6 | AMP-6T | Mini-Circuits | ZX60-24-S+ | 24 dB | 5,840 MHz | -16 dBm | Pass |
| 7 | AMP-7T | Adv. UWave | PA2403P | 30 dB | 5,840 MHz | 0 dBm | Pass |
| 8 | AMP-1R | RF Lambda | RLNA09G10G | 33 dB | 10,250 MHz | -70 dBm | Pass |
| 9 | AMP-2R | RF Lambda | RLNA04G08G | 44 dB | 5,840 MHz | -70 dBm | Pass |
| 10 | AMP-3R | Mini-Circuits | ZRL-2400LN+ | 32 dB | 1,020 MHz | -65 dBm | Pass |
| 11 | AMP-4R | Mini-Circuits | ZRL-700+ | 30 dB | 270 MHz | -54 dBm | Pass |
| 12 | AMP-5R | Mini-Circuits | ZFL-1HADB+ | 10 dB | 10 MHz | -1 dBm | Pass |

Table 5. RF filter test results.

| Item | Project Part Number | Manufac. | Manufacturer Part Number | Specified Frequency | Specified Bandwidth | Specified Insertion Loss | Test Pass / Fail |
|---|---|---|---|---|---|---|---|
| 1 | BP-1T | Reactel | 7CX11-1020-X200S11 | 1,020 MHz | 200 MHz | < 3 dB | Pass |
| 2 | BP-2T | Reactel | 4C3-10250-X200S11 | 10,250 MHz | 200 MHz | < 3 dB | Pass |
| 3 | BP-3T | Reactel | 4C2-5840-X200S11 | 5,840 MHz | 200 MHz | < 3 dB | Pass |
| 4 | BP-4T | Reactel | 8BMX-270-X30S11 | 270 MHz | 30 MHz | < 3 dB | Pass |
| 5 | BP-1R | Reactel | 4C3-10250-X200S11 | 10,250 MHz | 200 MHz | < 3 dB | Pass |
| 6 | BP-2R | Reactel | 4C2-5840-X200S11 | 5,840 MHz | 200 MHz | < 3 dB | Pass |
| 7 | BP-3R | Reactel | 7CX11-1020-X200S11 | 1,020 MHz | 200 MHz | < 3 dB | Pass |
| 8 | BP-4R | Reactel | 8BMX-270-X30S11 | 270 MHz | 30 MHz | < 3 dB | Pass |

Table 6. Oscillator test results.

| Item | Project Part Number | Manufac. | Manufacturer Part Number | Specified Frequency | Specified Power Output | Test Pass / Fail |
|---|---|---|---|---|---|---|
| 1 | PLL-1T | Wenzel Associates | 500-29608 | 750 MHz | 13 dBm | Pass |
| 2 | PLL-2T | Wenzel Associates | 500-29612 | 9,230 MHz | 13 dBm | Pass |
| 3 | PLL-3T | Wenzel Associates | 500-29611 | 4,820 MHz | 13 dBm | Pass |
| 4 | PLL-1R | Wenzel Associates | 500-29612 | 9,230 MHz | 13 dBm | Pass |
| 5 | PLL-2R | Wenzel Associates | 500-29611 | 4,820 MHz | 13 dBm | Pass |
| 6 | PLL-3R | Wenzel Associates | 500-29608 | 750 MHz | 13 dBm | Pass |

# CHAPTER 6. CONCLUSIONS

This initial project was successful in completing the first four tasks of the original scope, including the research and literature search, the design, procurement of equipment and materials, construction, and subsystem testing. The original project scope included the follow-on tasks of integration and field testing, but working with FDOT, it was determined that this initial project should be rescoped and considered completed after the subsystem testing task. The original project schedule was impacted by procurement delays and an underestimate of the amount of time necessary for undergraduate student researchers to construct the sophisticated and complex microwave test stations. In addition, at the start of the project, the plan was to use two FDOT trailers for the portable test stations. Several years after the start of the project, one of the trailers was no longer available when the mobile station integration work was to begin. To continue would have required the research team to identify another FDOT trailer asset and redesign that station for that new trailer. The final reason it was decided to split the project into this initial project and a future project was that the University of North Florida instituted travel bans for faculty and student researchers in early 2020 during the pandemic. This created an indefinite delay on the project as the five-year FDOT project maximum limit of early 2021 was approaching.

A future research project will be proposed to the FDOT to complete the project by first integrating the transmitter and receiver systems into the microwave test stations, and then conducting the field tests with the transmitter microwave test station positioned in the lower Florida Keys and the receiver microwave test station positioned near the western end of the Florida Panhandle. It is hoped a radio link will be established between the two sites that is of sufficient reliability to warrant building a permanent link and interconnecting with the existing statewide network.

REFERENCES

Anderson, K., Doss-Hammel, S., & Frederickson, P. (2003). Microwave and Infrared Propagation Over the Sea during The Rough Evaporation Duct (RED) Experiment. *IEEE Military Communications Conference*, Boston, pgs. 1416-1421.

Babin, S. M., Young, G. S., & Carton, J. A., (1997). A New Model of the Oceanic Evaporation Duct, *Journal of Applied Meteorology*, Volume 36, Issue 3, pgs. 193-204

Dinc, E., & Akan, O. B. (2014). Beyond-Line-of-Sight Communications with Ducting Layer. *IEEE Communications Magazine*, Volume 52, Issue 10, pgs. 37-43.

Frederickson, P. A., (2012). Improving the Characterization of the Environment for AREPS Electromagnetic Performance Predictions. *Weather Impacts Decision Aids Workshop*, Reno, NV, pgs. 6-8.

Gadwal, V., & Barrios, A., (2009). Channel Modeling Using the Parabolic Equation for RF Communications. *IEEE Military Communications Conference*, Boston, pgs. 456-461.

Hansen, H. J., Kulessa, A. S., Marwood, W., Forrest, M., Borg, D., & Reinhold, O., (2011). Multipath and anomalous propagation studies of Ka band emissions using a distributed transmit-receive radio link network experiment. *Proceedings of the Asia-Pacific Microwave Conference*, Melbourne, pgs. 749-752.

Kerans, A. J., Kulessa, A. S., Woods, G. S., & Clark, A. J., (2010). A Theoretical Path Design for Long Range Over Ocean Microwave. *Proceedings of the IEEE Oceans Conference*, Sydney Australia, pgs. 1-4.

Luddy, M. J., Winters, J. H., & Lackpour, A., (2011). Beyond Line-of-Sight Communications with Smart Antennas. Proceedings of the American Society of Naval Engineers, *Intelligent Ships Symposium IX*, Philadelphia, pgs. 891-895.

Ozgun, O., Apaydin, G., Kuzuoglu, M., & Sevgi, L. (2011). PETOOL: MATLAB-Based One-Way and Two-Way Split-Step Parabolic Equation Tool for Radiowave Propagation over Variable Terrain. *Computer Physics Communications*, pgs. 2638-2654.

Patterson, W. L. (2007). Advanced Refractive Effects Prediction System (AREPS). *IEEE Radar Conference*, Boston, pgs. 891-895.

Rottier, J. R., Rowland, J. R., Konstanzer, G. C., Goldhirsh, J., & Dockery, G. D., (2001). APL Environmental Assessment for Navy Anti-Air Warfare. *Johns Hopkins Applied Physics Laboratory Technical Digest*, Volume 22, Issue 4, pgs. 447-461.

Woods, G. S., Ruxton, A., Huddlestone-Holmes, C., & Gigan, G. (2009). High-Capacity, Long-Range, Over-Ocean Microwave Link Using the Evaporative Duct. *IEEE Journal of Oceanic Engineering*, Volume 34, Issue 3, pgs. 323-330.

Yang, S., Kunde, Y., Yixin, Y., & Yuanliang, M., (2015). A New Evaporation Duct Climatology over the South China Sea. *Journal Of Meteorological Research*, Volume 29, Issue 5, pgs. 764-778.

APPENDIX 1. TEST PROCEDURES

## A1.1 AMPLIFIER TEST PROCEDURES

There are 12 amplifiers in the design. The high frequency transmitter test station amplifiers, AMP-5T and AMP-7T were tested separately from the other 10 amplifiers. Their high frequency operation required a special test layout shown in Figure A1. The procedures for testing these two amplifiers are shown in Table A1. For the remaining ten amplifiers the test procedures are more simple and are shown in Table A2.

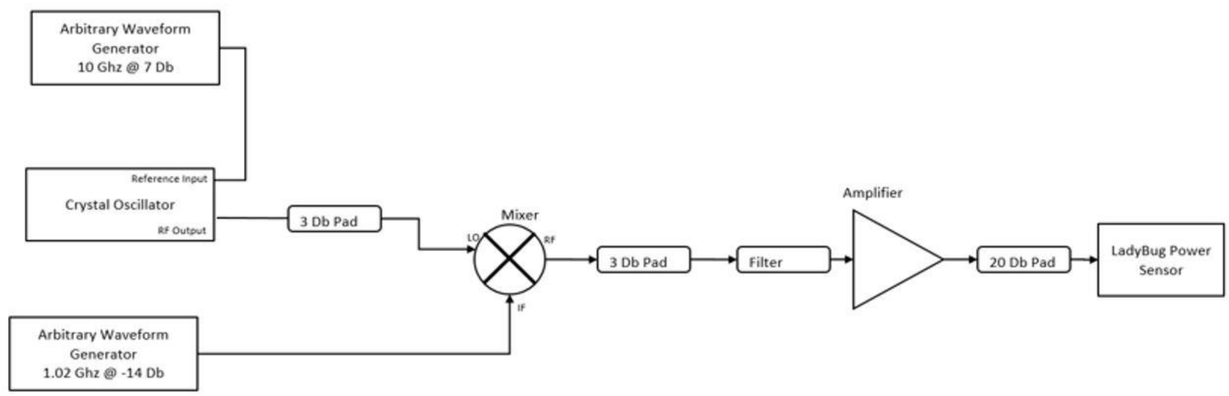


Figure A1. High frequency amplifier test layout.

Table A1. High frequency amplifier test procedures.

| Procedure Number | High-Frequency Amplifier Test Procedure |
|---|---|
| 1 | Connect Rigol frequency generator (1) RF output to IF input of mixer. |
| 2 | Connect Rigol frequency generator (2) to reference input of PLL. |
| 3 | Connect output of PLL to a 3 dB attenuator. |
| 4 | Connect output of attenuator to LO input of mixer. |
| 5 | Connect RF output of mixer to 3 dB attenuator. |
| 6 | Connect output of attenuator to 10,250 MHz filter. |
| 7 | Connect output of filter to DUT. |
| 8 | Connect output of DUT to 20 dB attenuator. |
| 9 | Connect output of attenuator to Signal Hound frequency analyzer. |
| 10 | Connect Signal Hound frequency analyzer to PC through USB. |
| 11 | Ensure there is nothing connected to power supply. |
| 12 | Determine input voltage required for both DUTs (PLL and Amplifier.). |
| 13 | Turn on power supply and set the voltage. |
| 14 | Turn off power supply. |
| 15 | Connect power supplies to respective loads. (PLL and LNA). |
| 16 | Launch Signal Hound software and wait until loaded. |
| 17 | Choose appropriate reference frequency and 1 dB compression point from datasheet and enter values into the Rigol Frequency Generator (1). |
| 18 | Choose appropriate reference frequency and 1 dB compression point from datasheet and enter values into frequency generator (2). |
| 19 | Double-check to ensure all components are correctly connected. |
| 20 | Turn on power supplies. |
| 21 | Press the “RF” softkey on Rigol frequency generator to enable signal. |
| 22 | Press the “RF” softkey on frequency generator 2. |
| 23 | Navigate to frequency analysis. |
| 24 | Determine gain of amp by taking amplifier out of circuit and measured receive power without amp. Then put amp in and measured receive power (less negative). Difference between two is gain. Compare results with test specification. |
| 25 | Press the “RF” softkey on Rigol frequency generator to disable signal. |
| 26 | Press the “RF” softkey on frequency generator 2 to disable signal. |
| 27 | Power down power supplies. |
| 28 | Power down Signal Hound software. |
| 29 | Disconnect DUT from test setup. |

Table A2. Standard amplifier test procedures.

| Procedure Number | High-Frequency Amplifier Test Procedure |
|---|---|
| 1 | Connect Rigol frequency generator RF output to male-to-male SMA “bullet”. |
| 2 | Ensure 20 dB attenuator is within test setup. |
| 3 | Connect 20 dB Attenuator to LadyBug power sensor. |
| 4 | Connect LadyBug Power Sensor to PC through USB. |
| 5 | Ensure there is nothing connected to power supply. |
| 6 | Determine input voltage required for DUT. |
| 7 | Turn on power supply and set the voltage. |
| 8 | Turn off power supply. |
| 9 | Connect power supply to DUT. |
| 10 | Launch LadyBug power sensor software. |
| 11 | Choose appropriate reference frequency and 1-dB compression point from datasheet, and enter values into the Rigol frequency generator. |
| 12 | Double-check to ensure all components are correctly connected. |
| 13 | Press the “RF” softkey on Rigol frequency generator to enable signal. |
| 14 | Note the value that appears on the LadyBug software. Compare results with test specification. |
| 15 | Press the “RF” softkey on Rigol frequency generator to disable signal. |
| 16 | Power down power supply. |
| 17 | Power down LadyBug software. |
| 18 | Power down Rigol frequency generator. |
| 19 | Disconnect DUT from test set-up. |

## A1.2 RF FILTER TEST PROCEDURES

There are three parts to the test procedures for testing the eight subsystem RF filters. The test parts are shown in Tables A3, A4, and A5.

Table A3. RF filter test procedure part 1: Calibration.

| Procedure Number | RF Filter Test Procedure Part 1: Calibration |
|---|---|
| 1 | Connect Rigol frequency generator RF output to male to male SMA “bullet”. |
| 2 | Connect “bullet” to SMA connector of Signal Hound spectrum analyzer. |
| 3 | Connect Signal Hound frequency analyzer to PC through USB. |
| 4 | Launch Signal Hound software and wait until loaded. |
| 5 | Choose appropriate reference frequency and 1-dB compression point from datasheet, and enter values into the Rigol frequency generator. |
| 6 | Double-check to ensure all components are correctly connected. |
| 7 | Press the “RF” softkey on Rigol frequency generator to enable signal. |
| 8 | Navigate to network analysis. |
| 9 | Click Run Sweep. software is now calibrated. |
| 10 | Press the “RF” softkey on Rigol frequency generator to disable signal. |

Table A4. RF filter test procedure part 2: Frequency and Bandwidth.

| Procedure Number | RF Filter Test Procedure Part 2: Frequency and Bandwidth |
|---|---|
| 1 | Replace “bullet” with DUT (Filter). |
| 2 | Using the Signal Hound software, navigate to the center frequency and enter the desired frequency found either on the part number of the DUT or the associated datasheet. |
| 3 | Enter the appropriate step bandwidth. |
| 4 | Choose appropriate Reference frequency and 1-dB compression point from datasheet and enter values into the Rigol frequency generator. |
| 5 | Double-check to ensure all components are correctly connected. |
| 6 | Press the “RF” softkey on Rigol frequency generator to enable signal. |
| 7 | Click Run Sweep. |
| 8 | Use the controls to find the max peak and note this peak. |
| 9 | Use the delta controls within the same cluster to find the delta bandwidth by dragging one to each side of the band drop of the filter. Note this frequency. Compare results with test specification. |
| 10 | Note dB level (top right of graph). This can be used for the insertion loss test if need be. |
| 11 | Press the “RF” softkey on Rigol frequency generator to disable signal. |
| 12 | Power down Signal Hound software. |
| 13 | Power down Rigol frequency generator. |
| 14 | Disconnect DUT from test setup. |

Table A5. RF filter test procedure part 3: Insertion Loss.

| Procedure Number | RF Filter Test Procedure Part 5: Insertion Loss |
|---|---|
| 1 | Connect Rigol frequency generator RF output to male to male SMA “bullet”. |
| 2 | Ensure 20 dB attenuator is within test set-up. |
| 3 | Connect 20 dB attenuator to LadyBug power sensor. |
| 4 | Connect LadyBug power sensor to PC through USB. |
| 5 | Launch LadyBug power sensor software. |
| 6 | Choose appropriate reference frequency and 1 dB compression point from datasheet and enter values into the Rigol frequency generator. |
| 7 | Double-check to ensure all components are correctly connected. |
| 8 | Press the “RF” softkey on Rigol frequency generator to enable signal. |
| 9 | Note the value that appears on the LadyBug software. Compare results with test specification. |
| 10 | Press the “RF” softkey on Rigol frequency generator to disable signal. |
| 11 | Power down LadyBug software. |
| 12 | Power down Rigol frequency generator. |
| 13 | Disconnect DUT from test setup. |

A1.3 OSCILLATOR TEST PROCEDURES

For the subsystem oscillators there are three parts to the test procedures. These three parts are shown in Tables A6, A7 and A8.

Table A6. Oscillator test procedure part 1: Calibration.

| Procedure Number | Oscillator Procedure Part 1: Calibration |
|---|---|
| 1 | Connect Rigol frequency generator RF output to male to male SMA “bullet”. |
| 2 | Connect “bullet” to 20 dB attenuator. |
| 3 | Connect 20 dB attenuator to SMA connector of Signal Hound frequency analyzer. |
| 4 | Connect Signal Hound frequency analyzer to PC through USB. |
| 5 | Launch Signal Hound Software and wait until loaded. |
| 6 | Choose appropriate reference frequency and 1-dB compression point from datasheet and enter values into the Rigol frequency generator. |
| 7 | Double-check to ensure all components are correctly connected. |
| 8 | Press the “RF” softkey on Rigol frequency generator to enable signal. |
| 9 | Navigate to frequency analysis. |
| 10 | Click Run Sweep. software is now calibrated. |
| 11 | Press the “RF” softkey on Rigol frequency generator to disable signal. |

Table A7. Oscillator test procedure part 2: Frequency.

| Procedure Number | Oscillator Procedure Part 2: Frequency |
|---|---|
| 1 | Replace “bullet” with DUT (Filter). |
| 2 | Using the Signal Hound software, navigate to Center frequency and enter the desired frequency found either on the part number of the DUT or the associated datasheet. |
| 3 | Enter the appropriate step bandwidth. |
| 4 | Choose appropriate reference frequency and 1-dB compression point from datasheet and enter values into the Rigol frequency generator. |
| 5 | Double-check to ensure all components are correctly connected. |
| 6 | Press the “RF” softkey on Rigol frequency generator to enable signal. |
| 7 | Click Run Sweep. |
| 8 | Use the controls to find the max peak and note this peak. |
| 9 | Use the delta controls within the same cluster to find the delta bandwidth by dragging one to each side of the band drop of the filter. Note this frequency. Compare results with test specification. |
| 10 | Press the “RF” softkey on Rigol frequency generator to disable signal. |
| 11 | Power down Signal Hound software. |
| 12 | Power down Rigol frequency generator. |
| 13 | Disconnect DUT from test setup. |

Table A8. Oscillator test procedure part 3: Output level.

| Procedure Number | Oscillator Procedure Part 3: Output Level |
|---|---|
| 1 | Connect Rigol frequency generator RF output to male to male SMA “bullet”. |
| 2 | Ensure 20 dB attenuator is within test set-up. |
| 3 | Connect 20 dB attenuator to LadyBug power sensor. |
| 4 | Connect LadyBug power sensor to PC through USB. |
| 5 | Launch LadyBug power sensor software. |
| 6 | Choose appropriate reference frequency and 1-dB compression point from datasheet and enter values into the Rigol frequency generator. |
| 7 | Double-check to ensure all components are correctly connected. |
| 8 | Press the “RF” softkey on Rigol frequency generator to enable signal. |
| 9 | Note the value that appears on the LadyBug software. Compare results with test specification. |
| 10 | Press the “RF” softkey on Rigol frequency generator to disable signal. |
| 11 | Power down LadyBug software. |
| 12 | Power down Rigol frequency generator. |
| 13 | Disconnect DUT from test setup. |